91602
new 82-10

ontario hydro
research division

COMPLIMENTARY COPY
Please Credit Ontario Hydro Research if
Reproduced in Whole or in Part

AUTOMATIC GENERATION CONTROL AND GOVERNOR TESTS AT SIR ADAM BECK II GS

Report No 87-219-K

G.R. Bérubé
Engineer
System Studies Section

ABSTRACT

Tests were conducted at S.A. Beck II GS (SAB II) to study the performance of individual units and the overall plant under Automatic Generation Control (AGC). At the same time measurements were made of various governor and turbine parameters. Based on the results of these tests a dynamic model for the components of the AGC and governing system at SAB II has been produced.

Observations are made on abnormalities in the operation of the AGC plant hardware noted during the performance of these tests.

job	file	date	report no.
18-386-022	813.22	August 27, 1987	87-219-K

TABLE OF CONTENTS

		Page
1.0	BACKGROUND	1
1.1	AGC Simulator	2
2.0	BECK II GS GOVERNORS AND AGC PLANT HARDWARE	2
2.1	SAB II AGC Hardware	2
2.2	Woodward Governors	3
2.3	SAB II GS Turbines and Penstocks	3
3.0	INSTRUMENTATION AND TEST MEASUREMENTS	3
4.0	TEST RESULTS	4
4.1	AGC Control Hardware Tests	4
4.1.1	Motor Operated Setter(MOS) and Transmitters	5
4.1.2	EHT Response	6
4.2	Governor/Turbine Tests	7
4.2.1	Static Measurements	7
4.2.2	Gate Travel Tests	8
4.2.3	Open and Closed Loop Responses	8
4.2.3.1	Servomotor Open Loop Gain, $1/T_g$	9
4.2.3.2	Closed Loop Response	10
4.2.4	Water Starting Time, T_w	10
4.3	Watt Transducers	11
4.4	Overall Performance	11
5.0	MODELING AND SIMULATION	12
5.1	Simulations	12
5.1.1	EHT Step Tests	12
5.1.2	AGC Open Loop Tests	12
5.2	Governor Modeling	13
6.0	OBSERVATIONS ON PERFORMANCE OF AGC SYSTEM AT SAB II	13
6.1	AGC Control Pulses	13
6.2	Effect of Speed Setting on EHT Gain	14
7.0	SUMMARY AND CONCLUSIONS	15
7.1	Acknowledgments	15
REFERENCES		16
TABLES		
1.	Model Parameters for SAB II AGC Hardware and Governors	17
2.	SAB II AGC Open Loop Response Test Results	18
3.	SAB II GS Governor Mechanical Settings (March 1987)	19
4.	Measured Parameter Values for SAB II AGC Hardware and Governors	20
5.	"TYPE 10" and "HYGOV" Model Parameters for SAB II Governors	21

TABLE OF CONTENTS (cont'd)

APPENDIX 1 Transfer Functions for Hydraulic Governors

APPENDIX 2 Determination of Open Loop Gain

LIST OF FIGURES

1. Block Diagram Overview of AGC System for S.A.Beck II GS
2. Block Diagram Model for AGC Hardware
3. Schematic of Woodward Cabinet Actuator with Electro-Hydraulic Transducer
4. Block Diagram Model for Governor and Turbine
5. AGC Open Loop Test - Raise Output 100%/min. for Thirty Seconds
6. Electro-Hydraulic Transducer Calibration Curves
7. Magnetic Amplifier Frequency Response
8. Electro-Hydraulic Transducer Frequency Response
9. Magnetic Amplifier Input Current vs. Gate Position
10. Electro-Hydraulic Transducer Step Input Tests
11. Speed Setter Static Calibration
12. Unit Power Output vs. Gate Position
13. Speed Droop Characteristic
14. Gate Travel Closing Test
15. Determination of Governor Open Loop Gain
16. Gate Frequency Response
17. Gate Travel Tests - Determination of Water Time Constant
18. Watt Transducer Transfer Function Block Diagram
19. AGC Closed Loop Test
20. AGC Closed Loop Test
21. Electro-Hydraulic Transducer Step Input Test Simulation - 10% Closing Step
22. Electro-Hydraulic Transducer Step Input Test Simulation - 100% Opening Step
23. Electro-Hydraulic Transducer Step Input Test Simulation - 100% Closing Step
24. AGC Open Loop Test Simulation
25. Simplified Overall Model Block Diagram for AGC Hardware and Governor
26. Recorded AGC Operation

91602
new 82-10

ontario hydro
research division

To: Dr. D. Mills
Director of Research

AUTOMATIC GENERATION CONTROL AND GOVERNOR TESTS AT SIR ADAM BECK II GS

G.R. Bérubé

Tests were conducted at S.A. Beck II GS (SAB II) to study the performance of individual units and the overall plant under Automatic Generation Control (AGC). At the same time measurements were made of various governor and turbine parameters. Based on the results of these tests a dynamic model for the components of the AGC and governing system at SAB II has been produced.

Observations are made on abnormalities in the operation of the AGC plant hardware noted during the performance of these tests.

1.0 BACKGROUND

Automatic Generation Control (AGC) provides automatic dispatching of generator unit outputs at selected controlled plants throughout Ontario. At any given time all or some of the available generating stations, Lakeview, SAB II, Des Joachims, Otto Holden and Lambton may be selected for automatic control. When selected, each controlled plant receives load control signals from the Richview System Control Centre (SCC) via microwave communication channels.

At SAB II sixteen 80 MVA units divided into two control groups are available for AGC. The turbines of each of these units are controlled by Woodward Cabinet Actuators. A transducer, included as part of the governing system, converts the load control signals received from Richview into a mechanical signal which produces changes to the turbine wicket gate position. For the normal operating range the unit generator output is linearly related to this wicket gate position.

job	file	date	report no.
18-386-022	813.22	August 27, 1987	87-219-K

1.1 AGC SIMULATOR

An AGC Simulation Program was developed to provide detailed off-line simulations of the real time AGC system. The intended uses of the simulator include studying various alternatives for future upgrades or modifications to the AGC system and performing assessments of alternative control strategies. Each controlled generating plant and its associated control hardware is included in the simulator in the form of a dynamic model.

Part of the development of the AGC simulator included a validation stage during which the simulator output was compared with actual AGC data recorded using the Data Acquisition and Computing System (DACS). Tests conducted with the SAB II plant on control, either alone or in combination with other controlled plants, produced unsatisfactory results. Discrepancies between the simulated results and actual AGC operation with SAB II on control appeared to be due to improper modeling of the control hardware for this plant.

Based on the above, at the request of the Power System Operations Division (PSOD), a number of tests were performed on the units and control hardware at SAB II to determine the static and dynamic performance of these devices. The results have been used to establish dynamic models appropriate for simulation of AGC operation at the plant and suitable for representing the dynamics of each individual unit during interconnected system operation.

2.0 BECK II GS AGC PLANT HARDWARE AND GOVERNORS

Section 2.1 provides a brief description of the various hardware components at SAB II and Richview SCC which provide AGC. A block diagram overview of the relationship between the various elements is included as Figure 1. A list of the parameters used in the models presented in this Section is provided as Table 1.

2.1 SAB II AGC HARDWARE

The major functional components of the SAB II AGC hardware (including hardware located at Richview SCC) are shown in Figure 2 and described in some detail in Reference 1.

Generation control signals are processed by a directional impulse adjusting type (DIAT) control system at the Richview SCC. When a generation change is to be initiated the DIAT controller issues raise and lower output pulses of varying widths corresponding to the desired loading rate. The characteristic of the DIAT controller is sketched in Figure 2. The pulses are transmitted to SAB II where they are integrated by a Motor Operated Setter (MOS). The dc voltage output of the MOS (0 to 100 mV) is fed to a pair of transmitters which produce equal current outputs. Each of the two transmitters produces eight equal output currents (1 to 5 mA) which are connected to the sixteen unit governors.

The cabinet actuator governors at SAB II are outfitted with an auxiliary control consisting of a magnetic amplifier and a fast-responding Electro-Hydraulic Transducer (EHT). The magnetic amplifier amplifies the currents received from the transmitter to a current level suitable for driving the EHT solenoid. Currents applied to the EHT solenoid result in small mechanical displacements (up to 3/8") of a piston which is attached to the speed setting linkages of the unit governor. The governor converts the displacement of the speed setting linkages to changes in the turbine wicket gate position and subsequently generator output. The functioning of the EHT is described in detail in Reference 2.

Tentative transfer functions for each of the AGC hardware components are shown in Figure 2. The final form of a suitable transfer function block diagram for the overall AGC control hardware is presented in Section 5.

2.2 WOODWARD GOVERNORS

The governors at SAB II are Woodward Cabinet Actuators [1]. A simplified schematic diagram of the governor is shown in Figure 3. Rotating flyballs (governor head) produce a mechanical displacement proportional to speed which is connected by a floating lever to a pilot valve plunger. Movement of this pilot valve plunger admits oil under pressure to a series of servomotors which provide hydraulic amplification and re-position the turbine wicket gates. Mechanical feedback between the wicket gates and the floating lever connected to the pilot valve is provided by two connections providing permanent and temporary speed droop. The compensating dashpot, which provides the temporary speed droop characteristic, is primarily intended to stabilize unit operation under isolated conditions and is partially bypassed for AGC operation.

A model suitable for simulating the operation of this type of governor in power system studies is shown in block diagram form in Figure 4 [4,5,6].

For interconnected operation (i.e. generator synchronized to interconnected system), under normal conditions, two methods may be used to adjust unit loading. First the governor speed setter, shown in Figure 3, may be manually or remotely adjusted, producing a mechanical signal applied to the floating lever and pilot valve. Second, as described in the previous section, the governor is outfitted with an EHT which converts the AGC signals into mechanical displacements of the upper floating lever (refer to Figure 3). The speed setter and EHT are included as inputs to the governor block diagram of Figure 4.

2.3 SAB II GS TURBINES AND PENSTOCKS

Numerous models of varying complexity exist for simulating the dynamic performance of the hydroturbine and penstock [7]. Some simplifications may be made in the model when considering interconnected system operation. For small deviations about a steady state operating point, when operating connected to a large system, turbine torque changes are produced mainly by changes in gate position since speed deviation is minimal and head is assumed to remain relatively constant. Under these conditions, and for the wicket gate openings between no-load and full-load, the turbine torque is linearly related to wicket gate position by the turbine gain A_t. The effect of water inertia is accounted for by the water time constant T_w and initial gate position g_0 in the transfer function included in Figure 4. This model assumes an ideal lossless turbine. The classical turbine-penstock transfer function is obtained by assuming the unit is at full-load, i.e. $g_0 = 1$. Under constant speed conditions the output torque and mechanical power, expressed in the per-unit system, may be equated, providing the desired output for the governor-turbine block diagram.

3.0 INSTRUMENTATION AND TEST MEASUREMENTS

The tests were performed during the nights of March 9, 10 and 11, 1987. During this entire period fifteen of the available sixteen generators at SAB II were in-service. Based on the objective of the testing, i.e. modeling the AGC control hardware and governor parameters pertinent to AGC operation, the following AGC signals were monitored:

- Raise/Lower output pulses received from Richview SCC
- Motor Operated Setter voltage output
- Transmitter current outputs for both groups

The primary test unit was G19. In addition, for selected tests, unit G18 was monitored to search for any dissimilarities in controlled unit responses. These adjacent units were selected because they belong to different control groups and are equipped with different manufacturers' generators: unit G18's magnetic amplifier is fed from transmitter 1 and has a Westinghouse generator while G19 is connected to transmitter 2 and has a CGE generator. For the primary test unit the following quantities were monitored:

- Magnetic amplifier input current
- EHT input (Magnetic Amplifier Output) current
- EHT plunger position
- Wicket gate position and velocity
- Generator power output
- Generator unit frequency

The magnetic amplifier input and output currents were monitored using current shunts installed for the tests while the transmitter output currents were measured across calibrated 10 Ω resistors included in the AGC hardware.

The EHT plunger position was monitored using a Linear Differential Voltage Transducer (LDVT) while the gate position was measured using a slidewire potentiometer and bridge arrangement. For both quantities an output was produced which was linearly related to position.

The following overall plant quantities were also monitored:

- Total plant power output (measured using existing DACS transducers)
- Forebay and tailrace elevations (monitored continuously on plant chart recorder)

As appropriate for each of the tests, selected quantities from amongst those parameters described above were connected to a pair of 6-channel direct writing recorders. Records on both the direct writing recorders were time-synchronized.

For some of the tests a special interface unit, supplied and connected by the plant P&C staff, was used to allow signals to be applied directly to the input of the EHT magnetic amplifier. The interface unit effectively disconnected the magnetic amplifier and EHT from the AGC transmitter and blocked the normal EHT plunger locking feature associated with this mode of operation.

4.0 TEST RESULTS

4.1 AGC CONTROL HARDWARE TESTS

Tests conducted on the AGC hardware were used to identify the calibration and time responses of:

- the control hardware which converts the DIAT pulses to continuous voltage and current signals, namely the MOS and transmitters,
- the test unit EHT and associated magnetic amplifier,
- the watt transducers used to relay the plant output level to Richview SCC.

4.1.1 Motor Operated Setter (MOS) and Transmitters

The input generation control pulses from Richview SCC are converted to a dc signal, suitable for input to the individual unit EHTs, by the MOS and transmitters. To test the calibration of these devices and the response of individual units to control pulses, SAB II was de-selected from normal AGC control at Richview SCC and test signals were transmitted corresponding to various loading rates. At the plant all units other than the two test units, G18 and G19, were individually de-selected from control. In this manner a wide range of loading rates were tested without producing large generation changes at the plant.

Figure 5 is a record of one of the AGC tests in which pulses corresponding to a loading rate of 100%/minute were applied for 30 seconds. Both transmitter outputs and the power outputs of the test units G18 and G19 were monitored during the AGC tests to investigate the symmetry of response of different units in different control groups. Examination of Figure 5 and the records of the other tests revealed the following:

- There is little discernible time delay between the receipt of the pulses from Richview SCC and the corresponding change in MOS output.
- No limits on the travel of the MOS were encountered during performance of these tests.
- On certain records there appeared to be a slight backlash in the MOS response (e.g. following a series of raise pulses the first lower pulse does not produce as large a change in MOS output as subsequent lower pulses). This effect appears to be very minor and intermittent and is therefore not included in the MOS model.
- The response of both transmitters is virtually identical. The transmitters respond very quickly to changes in the MOS output. Although not essential, a small time constant ($T_t \simeq .04$ seconds) may be used in modeling the dynamics of the transmitters.
- The test DIAT pulses, MOS response and transmitter response were identical in the raise and lower directions.

Table 2 contains a list of the various tests which were performed along with the steady state changes in the output of the MOS and Transmitters and the generated output of each of the units on control.

The ideal DIAT characteristic should produce pulses with widths linearly related to the desired loading rate. The results contained in Table 2 indicate that the DIAT gain (pulse width/loading rate) decreases slightly as the loading rate increases.

The MOS and transmitter gains are constant for a wide range of loading rates with values:

MOS gain $K_m = 2.7$ mV/sec

Transmitter gain $K_t = 0.325$ mA/mV

The transmitter gain referred to a single unit is determined by dividing the above value by a factor of eight. These gains may be used along with a transmitter time constant, T_t, of 0.04 seconds in the block diagram model of Figure 2.

During the performance of the first in this series of tests (-10%/minute for 3 minutes) it was noted that the change in output for unit G18 was substantially larger than that achieved by unit G19 even though the calibration of the EHTs for both units was virtually identical (see next section) and they were receiving identical input signals from the transmitters. Upon investigation it was found that the gate positions of the two units were different and the speed setting of unit G18 was manually adjusted to align the gate openings. G19 continued to exhibit lower gain than G18 throughout the tests despite numerous attempts to manually bring the units in line using the manual speed setter. Based on the above, it appears that the overall governing system gain was substantially different for the two units. The effect of initial speed setting on the overall response is discussed further in Section 6.

4.1.2 EHT Response

The EHTs undergo routine maintenance and calibration on an annual basis. The EHTs for units G18 and G19 were inspected by station P&C staff a few weeks prior to the tests. The calibration curves relating plunger travel to input current are shown in Figure 6. From these plots it can be seen that the static response of the two EHTs is virtually identical and linear over the range of input currents used with AGC.

To identify the magnetic amplifier and EHT time constants, frequency response and step tests were performed. For these tests the interface unit and a signal generator were used to introduce controlled inputs to the magnetic amplifier of the test unit.

For the frequency response measurements small amplitude sinusoids of frequencies between 0.008 and 8 Hz were applied to the magnetic amplifier input while the magnetic amplifier output and EHT plunger position were monitored. Figures 7 and 8 are plots of the measured and simulated amplitude and phase characteristics of the magnetic amplifier and EHT respectively. The time constants used to produce the simulated results were selected to match the measured frequency characteristics, particularly in the low frequency range pertinent to AGC operation. The amplitude responses have been normalized to represent unity gain at low frequencies. The gain of the EHT and magnetic amplifier were determined through examination of their time responses.

Six different sets of step tests were performed with different step input sizes in the raise and lower output direction. Figure 9 is a plot of the steady state values of gate and magnetic amplifier input current obtained following each of the step tests. The tight scatter of points in Figure 9 indicates that there is little discernible backlash or deadband in the linkages between the EHT plunger and the pilot valve plunger or in the pilot valve itself.

Using Figure 9, a combined gain term may be determined for the magnetic amplifier and EHT. Assuming a 4% speed droop characteristic the EHT plunger position may be calibrated in terms of per-unit speed. For simulation purposes this permits the output of the EHT model to be used directly as input to the governor model of Figure 4. The steady state gains between magnetic amplifier input and output and EHT plunger position are:

mag amp output / input	K_a = 72.2 mA/mA
EHT position / mag amp output	K_e = 1.17 x 10^{-3} inch/mA
	= 1.482 x 10^{-4} pu speed/mA

Combining these two gains,

EHT position(pu speed) / mag amp input	$K_a \cdot K_e$ = 0.0107 p.u. speed / mA

The step input tests were also used to investigate the time responses of the magnetic amplifier and EHT for widely varying input magnitudes and initial starting points in both the open and close directions. Figure 10 is a record of one of the step tests performed showing magnetic amplifier input and output, EHT plunger position, gate and unit power output.

The magnetic amplifier time constant, T_a, of 0.094 seconds determined from the frequency response measurements was in good agreement with the measured time domain results for different step input sizes in both directions in the range of magnetic amplifier input currents between 1 and 5 mA. Contrasting with this, the time response of the EHT varied significantly with the magnitude and direction of the change in input current. Referring to Figure 10 it can be seen that the EHT plunger follows a linear trajectory for most of its travel. Its response was found to be substantially slower than that predicted from the frequency response results, indicating that the plunger velocity is limited. Nevertheless for AGC operation, where the input currents to the magnetic amplifier change relatively gradually, the velocity limits are not reached and a time constant, T_e, of 0.3 seconds may be used to model the EHT's dynamic response.

No deadband or sticking was noted in any of the tests performed on the EHT.

4.2 GOVERNOR / TURBINE TESTS

Table 3 lists the mechanical governor settings for the two test units as found during the three day test period (Note: some information was provided by Station Mechanical Maintenance staff). The temporary droop settings included in the Table were derived based on the compensating crank setting and calibration curves provided in Reference 8. The permanent droop settings are the approximate values as read from a front panel dial on the cabinet actuator.

4.2.1 Static Measurements

In each of the following static tests measurements were made after the test unit had settled to steady state.

The test unit was disconnected from the system and measurements of unit frequency/speed were made while the speed changer setting was gradually increased in increments of 1/4%. Figure 11 plots the speed setter calibration curve for speed increments in both the increase and decrease directions. Rated speed for the SAB II units is 150 RPM. Examination of this Figure reveals that the speed setter is appropriately calibrated for the speed range of interest.

With the unit synchronized to the system and at zero gate the speed changer setting was manually increased in increments of 1/4% until the wicket gates were fully open. This procedure was then repeated in closing the gates. The values of wicket gate position, power, and speed setting were tabulated at each step.

Figure 12 shows the steady state power vs. gate relationship. From this graph it can be seen that the no-load gate is approximately 10% while full load (80 MW) is reached near 100% gate. The static power/gate characteristic is approximately linear for gate openings between 10% and 90%.

Figure 13 is a plot of the incremental permanent speed droop characteristic. This plot was determined from the on-line tests by combining the speed setting versus gate measurements in the gate closing directions, with the speed setting calibration curve of Figure 11. The incremental permanent speed droop is approximately linear for gate openings above 10% with a slope equal to -0.039 pu speed/pu gate (i.e. $\simeq$ 4% permanent droop). The similar droop curve obtained by using the measurements in the open direction produced a curve with identical slope

but offset from the curve in Figure 13. This offset was not due to speed sensitivity deadband but rather appeared to be due to backlash in the linkages connecting the speed setting dial to the floating lever.

The governor speed deadband was not determined during these tests due to the lack of sufficiently sensitive frequency measurements.

4.2.2 Gate Travel Tests

The gate limit dial on the cabinet actuator was used to produce large step changes to the position of the pilot valve plunger and subsequently wicket gates. With the unit initially operating at 100% gate the speed setter dial was used to introduce a gate opening signal and the gate limit was quickly reduced to zero gate. This procedure ensured that the gate limit stop arm was pressing down directly upon the pilot valve plunger quickly saturating the pilot valve as the gate limit was reduced to zero (refer to Figure 3). In this manner the effect of the droop feedback was bypassed and the wicket gates were forced to move at their maximum velocity for almost the entire range of travel. This test was repeated several times in both directions with gate opening being initiated by rapidly releasing the gate limit while a large opening signal was applied. The gate position, velocity and generator output were monitored with a chart recorder operating at a high speed to fully resolve the gate dynamics.

Figure 14 is a plot of the gate position and velocity for one of the gate closing tests. For modeling purposes the maximum gate velocities in the open and close directions are 8%/sec and 21%/sec respectively. For detailed models the gate cushioning apparent in Figure 14 may be modeled by imposing a gate velocity limit in the closing direction of approximately 2.5%/sec for gate openings below 12%.

Additional gate travel tests were performed to determine if initial gate position affected gate velocity achieved for equal pilot valve position movements. For this purpose the procedure described above was repeated with gate limit steps of only 10% of gate opening/closing being applied. For equal inputs, as determined by the steady-state change in gate position, the gate velocities achieved were approximately equal for various tests with initial gate openings in the range of 10% to 100%.

4.2.3 Open and Closed Loop Responses

The values of the various time constants appearing in the governor model block diagram of Figure 4 may be ascertained by examining the closed loop response of the governor wicket gates for various speed signal inputs. Examination of the closed loop transfer function helps in understanding how each parameter affects the overall governor response. Appendix I derives the complete and simplified closed loop transfer function for the hydrogovernor representation of Figure 4 [5]. The complete transfer function (omitting non-linearities due to wicket gate velocity and position limits) relating incremental changes of the wicket gate position, g, to incremental speed changes, n, has the form:

$$\frac{g(s)}{n(s)} = \frac{1 + T_r \cdot s}{T_p T_g T_r \cdot s^3 + T_g(T_p + T_r) \cdot s^2 + [T_g + T_r(\delta + \sigma)] \cdot s + \sigma} \qquad (1)$$

For cabinet actuator governors the time constant T_p, relating the position of the gate servomotor (distributing) valve to the pilot valve, is quite small. Its value is not readily measurable and since its effect on the overall performance of the governor, particularly for load maneuvering, is

minimal it is often neglected in modeling governor dynamics. However, for this simplification to be reasonable the value of T_p must be significantly less than the dashpot reset time T_r. For AGC operation, with the solenoid-actuated dashpot bypass opened, the dashpot reset time is extremely small to permit fast loading and unloading of the controlled unit. Under these conditions it may not be reasonable to completely eliminate T_p from Equation 1. Nevertheless the cubic term containing all three time constants may safely be omitted simplifying the transfer function to the quadratic form:

$$\frac{g(s)}{n(s)} = \frac{(1 + T_r \cdot s)/\sigma}{(T_g(T_p + T_r)/\sigma) \cdot s^2 + [(T_g + T_r(\delta + \sigma))/\sigma] \cdot s + 1} \qquad (2)$$

The response of this general form of transfer function in both the time and frequency domains can be readily determined for different values of the governor parameters permitting simple comparison of the model responses with measured responses.

4.2.3.1 Servomotor Open Loop Gain, $1/T_g$

The servomotor time constant or overall governor open-loop gain ($1/T_g$) may be determined by examining the gate velocities achieved for various magnitudes of step inputs applied to the pilot valve piston [5]. Examination of the governor model (refer to Appendix 2) reveals that with the feedback linkages removed (ie. $\delta = 0$, and $\sigma = 0$) the gate velocity will be equal to the magnitude of an applied speed step input multiplied by the open-loop gain.

This relationship holds true as long as the gate velocity limits are not reached in either direction. If the feedback linkages cannot be removed, the effect of the permanent and temporary droops must be accounted for in determining the open-loop gain from the gate velocity and speed step input (Appendix 2). An estimate for the open loop gain may be calculated from measurements of the maximum gate velocity achieved as soon as the gates begin to move.

For this test the interface unit and a signal generator were used to introduce controlled step inputs of various magnitudes to the EHT magnetic amplifier of the test unit. The EHT converted these steps into rapid displacements of the pilot valve piston. Figures 15(a) and (b) plot maximum gate velocity attained versus speed deviation for input steps in the open and close directions. The maximum gate velocity limit in the gate opening direction (0.08 pu/sec) is clearly visible upon examination of Figure 15(b). The slope of the lines drawn through the measurements lying within the gate velocity limits may be used in estimating the value of T_g in both directions (Appendix 2);

$1/T_g$(open) = maximum gate velocity / step speed deviation

= (0.08 pu/sec) / (0.014 pu)

= 5.7 sec^{-1}

$1/T_g$(close) = (0.19 pu/sec) / (0.025 pu)

= 7.6 sec^{-1}

Differences in the performance of the governor in the two directions is to be expected and has been observed in previous testing [9]. The above values of $1/T_g$ are used as initial estimates of the

open-loop gain in the gate opening and closing directions. Simulations and comparisons with other test results, described in upcoming sections, are used to verify that these values for the open loop gain are reasonable.

4.2.3.2 Closed Loop Response

Measurements were carried out to determine the frequency response of the wicket gates to speed setting inputs applied by using the interface unit and the EHT. For these tests the initial gate position was approximately 65% and the magnetic amplifier input current magnitude was selected to produce a ±10% oscillation in the gate position at low frequencies. Measurements of magnitude and phase response for frequencies between 0.008 Hz and 8 Hz are plotted in Figures 16(a) and (b) respectively. Inputs of frequency above 0.8 Hz produced no appreciable wicket gate movement.

Using the known values of temporary and permanent speed droop and the estimates for open loop gain obtained in the previous section, the magnitude and phase of the transfer function of Equation 2 were calculated for various values of T_r and T_p. Good agreement with the measured results was obtained with values of T_r at 0.1 sec or less. As expected the value of T_p, within reasonable bounds, had little effect on the overall response. A simulated response providing a reasonably good fit to the measured parameters is included on Figure 16. (Note: The higher estimate of the open loop gain, $1/T_g$, produced the best results in fitting the frequency response data. The dual values of T_g are investigated further in an upcoming section through simulations of the time response tests conducted in both gate opening and closing directions.)

4.2.4 Water Starting Time, T_w

The effect of the water column inertia, as quantified by the water starting time, is readily observable when the gate position is changed rapidly. Because of inertia, for rapid increases in gate opening the mechanical output power dips slightly before increasing to its new steady state value. The reverse effect is observed when the gates are closed rapidly. In both cases the effect is most prevalent for large initial gate openings.

The gate travel tests described earlier were used to estimate the value of water starting time. The gate limit and speed setting controls on the cabinet actuator were used to introduce rapid 10% changes to the gate opening. The changes to generator output and gate position were recorded for a wide variety of initial gate positions. Figure 17 shows the gate and power output for 10% gate position changes in the open and close directions. Net head during this test was approximately 290 feet.

Simulated inputs corresponding to the gate position during the tests were applied to the turbine-penstock transfer function of Figure 4 and various values of T_w were tested to determine their effect on the power response. For the purpose of these simulations the generator electrical power output was assumed to be equal to the turbine mechanical power output after compensating for the watt transducer transfer function. A suitable value of T_w was determined to be approximately 1.2 seconds based on these simulations.

Although the classical turbine-penstock transfer function provided an acceptable match to observed conditions it is clear that a more detailed representation of the full turbine-penstock equations is required to simulate the power output accurately for rapidly changing gate positions. In particular for simulations of rapid movement of the gates over a wide range of gate position no value of T_w in the classical transfer function could reproduce the rapid power response which was observed. The differences between the simulated results and observed results is probably due to the small-signal assumptions used in linearizing the turbine-penstock dynamic equations. For

the purposes of modeling AGC operation, during which power changes are relatively slow, a simplified representation of the turbine-penstock equations should produce suitable results.

4.3 WATT TRANSDUCERS

The signals from individual watt transducers on each unit are combined to produce a total plant output signal. These transducers, while not part of the closed loop AGC system, are used to monitor the SAB II plant response to control signals; therefore, their response must be accounted for in determining the dynamics of the actual power changes occurring at the plant from the measured quantities.

Currently, Sangamo AW6S thermal converters are used to reproduce the total plant output signals for DACS. Figure 18(a) is a transfer function block diagram which may be used in simulating the response of these transducers. The transducers require approximately 5.5 seconds to respond to 90% of the applied step change in power.

New watt transducers, Scientific Columbus XL31K5A2-OH 2-element 3Ø 3-wire, have been installed and will eventually replace the existing transducers. These watt transducers were utilized to monitor the individual unit outputs of the two test units during the tests. Figure 18(b) shows the transfer function of this watt transducer determined through separate frequency response testing. The transducer settles to virtually its final value in approximately 200 ms.

4.4 OVERALL PERFORMANCE

To investigate the performance of the overall AGC closed loop system, tests were performed with SAB II selected for control on the AGC system. At Richview SCC, SAB II was selected as the only plant on control and the Area Control Error (ACE) deadband was reduced to 15 MW. This ensured that the AGC system would respond to small changes in the system generation and that all control signals would be sent to SAB II. At SAB II all in-service units were selected for control with the exception of G20.

The first test involved producing an undergenerated condition by rejecting G20 from full-load (80 MW). Figure 19 shows the plant output and AGC quantities during the test along with an event marker indicating the instant that the unit was rejected (note: the total plant output was measured with the existing slow transducers used by DACS). Within five seconds of tripping the unit a train of raise pulses were received which increased the total plant output by approximately 34 MW. Thirty seconds later (not shown on Figure 19) another series of raise pulses arrived which further increased the plant output by another 48 MW. It is unlikely that the second set of pulses was generated as a result of the generation rejection.

A second test was conducted by re-synchronizing G20 and rapidly raising its output to full-load using the speed setting and gate limit controls. The plant output and AGC quantities were recorded once again and are shown in Figure 20. As observed during previous tests, the unit requires approximately twelve seconds to reach its full output from the moment that the gate limit is released. A series of lower pulses was received sixteen seconds after the gate limit was released. The final plant output following these pulses was approximately 20 MW above its pretest value. Inspection of Figure 20 reveals that the pulses are not all received at equal one-second intervals and that the pulse widths vary over a wide range. These irregular lower pulses are discussed further in Section 6.

Both tests were repeated twice with varying results. With the ACE deadband reduced to only 15 MW the AGC signals, produced by ACE fluctuations due to other causes on the system, made it difficult to exactly pinpoint the signals which were produced as a direct result of the generation

reductions and increases at SAB II. Also the exact relationship between generation reductions/increases at SAB II and changes to the ACE was not established making it difficult to estimate what the exact inputs to the AGC system were during the tests.

5.0 MODELING AND SIMULATION

A summary of the model parameters determined in Section 4 is listed in Table 4.

5.1 SIMULATIONS

The AGC control hardware, governor and turbine-penstock models were combined and input to a continuous dynamic simulation software package. The simulated responses of the model were compared to the actual test results to demonstrate their validity.

5.1.1 EHT Step Tests

As described in Section 4 step changes to the magnetic amplifier input current were introduced using an interface unit and signal generator. For small steps, in which the steady state change in gate was ±20% or less, the simulated results were in good agreement with the observed results.

Figure 21 shows the simulated gate position and velocity and unit power output plotted along with the measured gate position for a 10% step test in the gate closing direction. For larger steps the EHT model had to be modified to include limits on the EHT plunger velocity. As discussed in Section 4 omitting the EHT plunger velocity limits from the AGC hardware model will have no effect on simulated results for the relatively slow loading and unloading associated with AGC operation.

Figures 22 and 23 show comparisons of simulated and test data for large magnetic amplifier step inputs in the open and close gate directions respectively. For the large opening step of Figure 22 the effect of gate velocity limit may be clearly seen from the velocity trace. For rapid gate travel in the closing direction a slight overshoot in gate position was observed in most of the test results. Also the measured gate velocity in the closing direction was significantly larger than the simulated value for large steps. No reasonable selection of parameters in the governor model reproduced the overshoot effect, however it was possible to increase the simulated gate velocity by increasing the open loop gain. The difference between the simulated and measured outputs for large gate excursions may be due to the small-signal assumptions used in deriving the simplified governor model. This should have no effect on the use of this model for simulating gate and power response to AGC signals.

In Figure 23 the effect of water inertia may be clearly seen in the power output increase which occurs as soon as the gates begin to close.

5.1.2 AGC Open Loop Tests

The AGC Open Loop tests in which various AGC pulse trains (corresponding to different loading rates) were transmitted from Richview SCC, were simulated to examine the model's operation under conditions which closely resemble those of normal AGC operation. The simulated pulses were directly reproduced through measurement of the actual pulse widths received during the test - i.e. the operation of the DIAT controller at Richview SCC was not included as part of these simulations.

The agreement between observed and simulated results was good in both the open and close directions for the various loading rates. Figure 24 (shown on three separate pages) shows all significant simulated and measured quantities for the thirty second application of the 100%/minute loading rate in the closing direction.

Even for modeling the fastest AGC loading rates it is clear that some of the models time constants in both the AGC hardware and governor models are not significant. Specifically, when the simplified model of Figure 25 was utilized to simulate the AGC Open Loop tests the simulated gate travel and power output were within one percent of the simulated values produced with the full model. Removal of the small time constants permits a much larger time step to be utilized in the numerical integration algorithms thus substantially reducing the simulation time.

The results in the open and close gate tests revealed that for the purpose of AGC simulations the lower value for the governor open-loop gain, $1/T_g = 5.7\ sec^{-1}$, produced adequate results in both directions.

5.2 GOVERNOR MODELING

The "TYPE 10" model of the TSSIMU program and the "HYGOV" model of the PTI Power System Simulator package are two commonly used hydraulic governor model formats. The "TYPE 10" model is intended for use in simulations of governors which utilize gate feedback to provide speed droop and is therefore essentially the same as the block diagram governor model of Figure 4. Table 5 summarizes the "TYPE 10" parameters which can be used in modeling the SAB II governor dynamics for interconnected system operation.

The "HYGOV" model is intended for governors which utilize pilot servomotor feedback to provide speed droop. Under certain conditions, the "HYGOV" parameters may be selected to provide a reasonable approximation of the dynamics of governors which employ gate feedback. However, under bypassed conditions when the dashpot reset time, T_r, is of the same order of magnitude as the distributing valve and gate servomotor time constant, T_g, the "HYGOV" model is not appropriate for modeling gate feedback governors such as the Woodward Cabinet Actuator. Appropriate "HYGOV" parameters for non-bypassed operation are included in Table 5.

6.0 OBSERVATIONS ON PERFORMANCE OF AGC HARDWARE

Some inconsistencies were noted in the operation of the AGC system at SAB II during the performance of these tests. Under certain circumstances these problems could lead to significant differences between the operation of specific components of the AGC system and the simulated response of the models for the AGC control hardware and governors.

6.1 AGC CONTROL PULSES

As noted during the performance of the closed loop AGC tests (refer to Section 4.4) the train of pulses received from Richview SCC were not evenly spaced at one second intervals and a number of unusually wide pulses were noted. This effect occurred most often in the lower output direction. Inspection of Figure 20 reveals that the train of normal pulses is interspersed with numerous unsynchronized wide pulses. During the tests it was confirmed that this effect was not caused by sticking relays at SAB II and that the undesirable pulses were present at the AGC receivers.

To confirm that this problem did not only occur during the controlled test the recorders were left on several times while SAB II was on AGC during morning pickup. Unequally spaced wide pulses were observed in almost every group of lower output pulses received. Figure 26 shows a typical group of pulses observed on the morning of March 10,1987.

Because of the relatively large width of these pulses they may contribute significantly to the change in output of the MOS and subsequently plant power output despite the infrequency of their occurrence. As an example of this effect the results of the closed loop test shown in Figure 20 were analyzed to determine the contribution of the unsynchronized pulses. By measuring the large changes in the MOS and Transmitter outputs produced by the wide pulses it is clear that over a third of the total output change was due to these pulses. Examination of several records revealed a wide variation in the number and size of the undesirable pulses. Nevertheless, it is clear that at certain times they may have a significant impact on the response of the AGC system. In particular since these pulses occur almost exclusively during receipt of the lower signals they may produce a substantial imbalance in the apparent gain of the AGC system in the raise and lower output directions.

It was not possible from the results of these tests or through subsequent investigations to determine the specific cause of this problem. It was noted that during the performance of the open loop tests, in which several trains of raise and lower pulses of different widths were transmitted from Richview SCC, only the first pulse in each group was non-uniform.

6.2 EFFECT OF SPEED SETTING ON EHT GAIN

Testing revealed that varying the speed setting on the cabinet actuator resulted in a change in the gain exhibited by the EHT to signals received from the control hardware (i.e. K_e calibrated in pu speed/mA). For different speed settings identical displacements of the EHT plunger produced different displacements of the pilot valve plunger and subsequently different changes to the gate position. The reason for the observed changes was not determined. The manual speed setter and EHT are both connected to fixed pivot points on the floating lever and therefore their gain relative to the pilot valve plunger should be a constant value.

The effect described above was particularly obvious during the first of the series of open loop tests when unit G18's response was nearly double that of the adjacent test unit to identical transmitter input signals despite having virtually identical permanent speed droop settings. Adjusting G18's speed setting to manually equalize the gate position of the two units improved the situation for subsequent tests however some imbalance remained.

At any given time this irregularity may change the effective gain of a number of units at the plant. Given the large number of connected units which are usually selected for AGC operation the overall effect on total plant gain should be minimal. One method which could be used to mitigate this problem would be to balance individual unit outputs and meet AGC loading requirements via a dedicated controller located at the plant.

7.0 SUMMARY AND CONCLUSIONS

1) Models suitable for simulating the dynamic response of the AGC Control Hardware and governing system at SAB II have been determined.

2) Discrepancies between measured and simulated results obtained with the AGC simulator may have been due to the occurrence of unsynchronized lower output pulses produced on the actual AGC system. This phenomenon should be investigated further to determine the source of the problem.

3) Consideration should be given to implementing a local controller to maintain individual unit output balance during AGC operation of the SAB II plant.

7.1 ACKNOWLEDGEMENTS

I wish to thank Mr. Banty Tezazu of PSOD for his invaluable assistance in coordinating the tests with the Control Centre staff. Also special thanks to Mr. John Newbold and the SAB II P&C staff and Mr. Colin Barnstone of the Mechanical Maintenance group for their help in instrumenting the various electrical and mechanical quantities at the plant. The expert advice of Mr. Gerry Manchur of the System Studies Section is gratefully acknowledged.

Approved:

David A. Lee

A.F. Baljet
Manager
Electrical Research Department

Submitted:

Roger Bérubé

G.R. Bérubé
Engineer
System Studies Section

REFERENCES

1. Y.L. Chan, "AGC Hardware at Richview SCC and Controlled Plants", Relay and Communications Dept. Report, November 1984.

2. Woodward Governing Company, "The Woodward Rapid Load Control Auxiliary", Woodward Bulletin 0702C.

3. Woodward Governor Company, "Cabinet Actuator for Governing Hydraulic Turbines", Woodward Bulletin 07004C.

4. IEEE Committee Report, "Dynamic Models for Steam and Hydro Turbines in Power System Studies", IEEE Trans. on Power Apparatus and Systems, Vol. PAS-92, pp. 1904-1915, Nov-Dec 1973.

5. D.G. Ramey and J.W. Skooglund, "Detailed Hydrogovernor Representation for System Stability Studies", IEEE Trans. on Power Apparatus and Systems, Vol. PAS-89, pp. 106-112, Jan 1970.

6. J.M. Undrill and J.L. Woodward, "Nonlinear Hydro Governing Model and Improved Calculation for Determining Temporary Droop", IEEE Trans. on Power Apparatus and Systems, Vol. PAS-86, pp. 443-452, April 1967.

7. R. Oldenburger and J. Donelson, "Dynamic Responses of a Hydro Electric Plant", AIEE Transactions, Vol. 81, pp. 403-419, October 1962.

8. J.P. Bayne, "Governor Settings in the Northwest Region", Ontario Hydro Research Division Report No. 77-118-H, March 1977.

9. K.R. McClymont, "Tests on Woodward Transducer", Ontario Hydro Research Report No. 57-422, October 1957.

TABLE 1

MODEL PARAMETERS FOR SAB II AGC HARDWARE AND GOVERNORS

Parameter	Description
K_m	Motor Operated Setter Gain (mV/sec)
K_t, T_t	Transmitter Gain (mA/mV) and Time Constant (sec)
K_a, T_a	Magnetic Amplifier Gain (mA/mA) and Time Constant (sec)
K_e, T_e	Electro-Hydraulic Transducer Gain (Inch/mA) and Time Constant (sec)
T_p	Pilot Valve and Servomotor Time Constant (sec)
$1/T_g$	Governor Open Loop Gain (pu gate/pu speed • sec)
r_{max}	Maximum Gate Velocity - Opening (pu gate/sec)
r_{min}	Maximum Gate Velocity - Closing (pu gate/sec)
g_{FL}	Full-Load Gate Position (pu)
g_{NL}	No-Load Gate Position (pu)
g_0	Initial Gate Position (pu)
σ	Permanent Speed Droop (pu speed/pu gate)
δ	Temporary Speed Droop (pu speed/pu gate)
T_r	Compensating Dashpot Reset Time (sec)
T_w	Water Time Constant (sec)
A_t	Turbine Gain (pu torque/pu gate) = $1/(g_{fl}-g_{nl})$

TABLE 2

BECK AGC OPEN LOOP RESPONSE TEST

Loading Rate (% Output/ minute)	Duration (minutes)	DIAT Pulse Width (sec)	MOS Output[1] (mV)	Transmitter[2] Output (mA)	Generator Output[3] G18 Δ(MW)	G18 Δ (%)	G19 Δ(MW)	G19 Δ (%)
+ 10%	3	0.05	+ 26.0	+ 8.5	+ 15.0	(+ 19%)	+ 16.8	(+ 21%)
- 10%	3	0.05	n/a	n/a	- 28.8	(- 36%)	- 16.8	(- 21%)
+ 20%	2	0.1	+ 31.0	+10.5	+ 30.0	(+ 37.5%)	+ 21.0	(+ 26%)
- 20%	2	0.1	n/a	-10.5	- 31.2	(- 39%)	- 21.0	(- 26%)
+ 30%	2	0.15	+ 46.0	+15.0	+ 45.6	(+ 57%)	+ 38.4	(+ 48%)
- 30%	2	0.15	n/a	-15.0	- 45.6	(- 57%)	- 38.4	(- 48%)
+ 50%	1	0.23	+ 37.0	+12.0	+ 42.0	(+ 52.5%)	+ 36.0	(+ 45%)
- 50%	1	0.23	- 36.8	-12.0	- 42.0	(- 52.5%)	- 36.0	(- 45%)
+100%	1/2	0.44	+ 36.0	+11.75	+ 39.6	(+ 49.5%)	+ 32.4	(+40.5%)
-100%	1/2	0.44	- 35.0	-11.25	- 38.4	(- 49.5%)	- 32.4	(-40.5%)

Notes:
1. Steady state change in MOS output - Output ranges between 0 and 100 mV.
2. Steady state change in both transmitter outputs - Output range between 8 and 40 mA corresponding to 1 to 5 mA per unit.
3. Steady state change in power output - percentages expressed in terms of 80 MW rated output.

n/a Measurement not available.

TABLE 3

BECK II GS GOVERNOR MECHANICAL SETTINGS (MARCH 1987)

	UNIT NO. G18	UNIT NO. G19
Upper Floating Lever Position	Inner Hole of 2	Inner Hole of 2
Restoring Ratio	38	40
Compensating Crank	4	5.5
Dashpot Needle Valve	1/8 turn open	1/8 turn open
Solenoid Actuated Dashpot Bypass Needle Valve	5 turns open	5 turns open
Temporary Droop	0.18	0.24
Permanent Droop	0.04	0.04

TABLE 4

MEASURED PARAMETER VALUES FOR SAB II AGC HARDWARE AND GOVERNORS

Governor and Turbine

σ = 0.04

δ = 0.24 (for unit G19 - normal setting for plant = 0.3)

g_{FL} = 1 pu

g_{NL} = 0.1 pu

r_{max} = + 0.08 pu/sec

r_{min} = - 0.21 pu/sec

1/Tg (open) = 5.7 sec^{-1}

(close) = 7.6 sec^{-1}

T_r = 0.1 sec

T_p = 0.04 sec

T_w = 1.2 sec

A_t = $1/(g_{FL} - g_{NL})$ = 1.11

AGC Hardware

K_m = 2.7 mV/sec

K_t = 0.325 mA/mV/8 (current to single unit)

K_a = 72.2 mA/mA

K_e = 1.17×10^{-3} inch/mA = 1.482×10^{-4} pu speed/mA

$K_{AGC} = K_m \cdot K_t \cdot K_a \cdot K_e$ = 0.074 inch/sec = 0.00117 pu speed/sec (overall gain)

T_a = 0.0936 sec

T_e = 0.3 sec

TABLE 5

"TYPE 10" AND "HYGOV" MODEL PARAMETERS FOR SAB II WOODWARD GOVERNORS

Description	TYPE 10[2]	HYGOV[2]
Servo System Gain	$Q = 5.7$	-
Servo System Time Constant	-	$T_g = 0.58$
Turbine Gain	-	$A_t = 1.11$
Permanent Droop	$R_p = 0.04$	$R = 0.04$
Temporary Droop[1]	$R_t = 0.3$	$r = 0.3$
Water Starting Time	$T_w = 1.2$	$T_w = 1.2$
Dashpot Reset Time (bypassed)	$T_r = 0.1$	-
(not bypassed)	- Not determined -	
Full Load Gate	$G_{FL} = 1$	-
No Load Gate (No Load Flow)	$G_{NL} = 0.1$	$q_{NL} \simeq 0.1$
Maximum Gate Limit	-	$G_{MAX} = 1$
Minimum Gate Limit	-	$G_{MIN} = 0$
Maximum Gate Opening Velocity	$R_{MAX(open)} = 0.08$	$R_{LIM} = \pm(0.08 + 0.21)/2$
Maximum Gate Closing Velocity	$R_{MAX(close)} = 0.21$	$R_{LIM} = \pm(0.08 + 0.21)/2$
Gate Buffer Region	$G_{BF} = 0.12$	-
Maximum Gate Closing Velocity in Buffer Region	$R_{BF(close)} = 0.025$	-
Deadband Magnitude	- Not determined -	
Power at Full Load Gate (pu on Gen. MVA Base)	$P_{MAX} = 1$	-

Notes : (1) Typical setting for units
(2) Blank fields indicate parameters not included in model

APPENDIX 1

TRANSFER FUNCTIONS FOR HYDRAULIC GOVERNORS

1. Governor Time Constants

A normal range of time constant values, for the type of hydraulic governor under consideration (see Figure 3), are listed below [4]:

1/(open loop gain) = T_g = 0.2 to 0.4 sec.

pilot valve time constant = T_p = 0.03 to 0.05 sec.

dashpot reset time = T_r = 2.5 to 25.0 sec.

The typical value of dashpot reset time is based on operation with a normal range of needle valve settings and no dashpot bypass activated. When the unit is used for generation control applications a dashpot bypass is activated which lowers the dashpot reset time permitting faster loading and unloading of the unit. A needle valve associated with the dashpot bypass is used to adjust the value of T_r. With this needle valve fully open the dashpot reset time may attain values as low as 0.1 second.

2. Open Loop Transfer Function

The open loop response of the governor may be used to determine the characteristics of the pilot and distributing valves and servomotors. The transfer function may be written directly in terms of the incremental speed deviation, n, and incremental gate deviation, g, by examining the block diagram of Figure 4 and ignoring the feedback branches corresponding to the compensating dashpot and permanent droop linkages of the governor.

$$\frac{g(s)}{n(s)} = \frac{1}{(1 + T_p \cdot s)T_g \cdot s} \qquad (1)$$

In Equation 1 and all subsequent transfer functions it is assumed that the gate travel is within the position and velocity limits thus eliminating these non-linearities from consideration. For most normal modes of operation the pilot valve time constant is insignificant. For these cases the open loop characteristics of the governor can be modeled with an integrator and the open loop gain, $1/T_g$.

3. Closed Loop Transfer Function - Permanent Feedback Only

Under certain conditions the closed loop response of the governor with only permanent feedback is of interest. This is the case when either the feedback linkage is disconnected, $\delta = 0$, or the dashpot is bypassed to the extent that the dashpot reset time is negligible, $T_r \approx 0$. Examining the block diagram of Figure 4 and omitting the pilot valve time constant the closed loop transfer function with permanent feedback only is written:

$$\frac{g(s)}{n(s)} = \frac{1/\sigma}{1 + (T_g/\sigma) \cdot s} \qquad (2)$$

4. Closed Loop Transfer Function - Permanent and Temporary Droop Feedback

Examining the block diagram of the hydraulic governor shown in Figure 4 [4,5] the overall closed loop transfer function may be written directly as:

$$\frac{g(s)}{n(s)} = \frac{1}{s \cdot T_g(1 + s \cdot T_p) + \sigma + (\delta T_r \cdot s / (1 + T_r \cdot s))} \qquad (3)$$

Multiplying out and grouping the various terms yields:

$$\frac{g(s)}{n(s)} = \frac{(1 + T_r \cdot s)}{T_p T_r T_g \cdot s^3 + T_g(T_p + T_r) \cdot s^2 + (T_g + T_r(\delta + \sigma)) \cdot s + \sigma} \qquad (4)$$

For time constant values in the normal range, the cubic term may be neglected without significantly altering the response of the overall transfer function in the usual frequency range of operation of the governor. Also since the value of T_p is usually negligible compared to T_r it is often omitted from the model and the transfer function. However, as previously discussed, for automatic load control applications the dashpot is bypassed permitting very small values of T_r to be attained. For these conditions the pilot valve time constant may be retained in the transfer function. The commonly used quadratic form derived by omitting the cubic term in Equation 2 is given below:

$$\frac{g(s)}{n(s)} = \frac{\frac{1}{\sigma}(1 + T_r \cdot s)}{\frac{T_g(T_r + T_p)}{\sigma} \cdot s^2 + \frac{T_g + T_r(\sigma + \delta)}{\sigma} \cdot s + 1} \qquad (5)$$

APPENDIX 2

DETERMINATION OF OPEN LOOP GAIN

Clearly the open loop gain could be most easily determined by removing both feedback linkages. For this configuration a given step speed input would produce a wicket gate velocity determined solely by the open loop gain and velocity limits. Referring to Equation 1 of Appendix 1 the expression for gate velocity may be written directly as:

for $n = N \cdot u(t)$

$$dg/dt = N/T_g \qquad (1)$$

where it has been assumed that the gates are stationary prior to the step speed input of magnitude N.

For the situation where the permanent feedback linkage is connected the closed loop transfer function is given by Equation 2 of Appendix 1. Again assuming a step speed input and zero initial gate velocity the gate velocity may be written as:

$$dg/dt = (N/T_g) \cdot e^{-\sigma t/T_g} \qquad (2)$$

The gate velocity measured at the moment the gates begin to move will still provide a reasonable means of calculating the open loop gain.

$$1/T_g = (dg/dt_{t=0})/N \qquad (3)$$

Addition of temporary droop feedback through the compensating dashpot linkage will result in a substantial decrease in the initial gate velocity due to the derivative action of this mechanism. For small values of the dashpot reset time the impact of this effect is limited and Eqn. 3 may still be used to produce an estimate of the open loop gain.

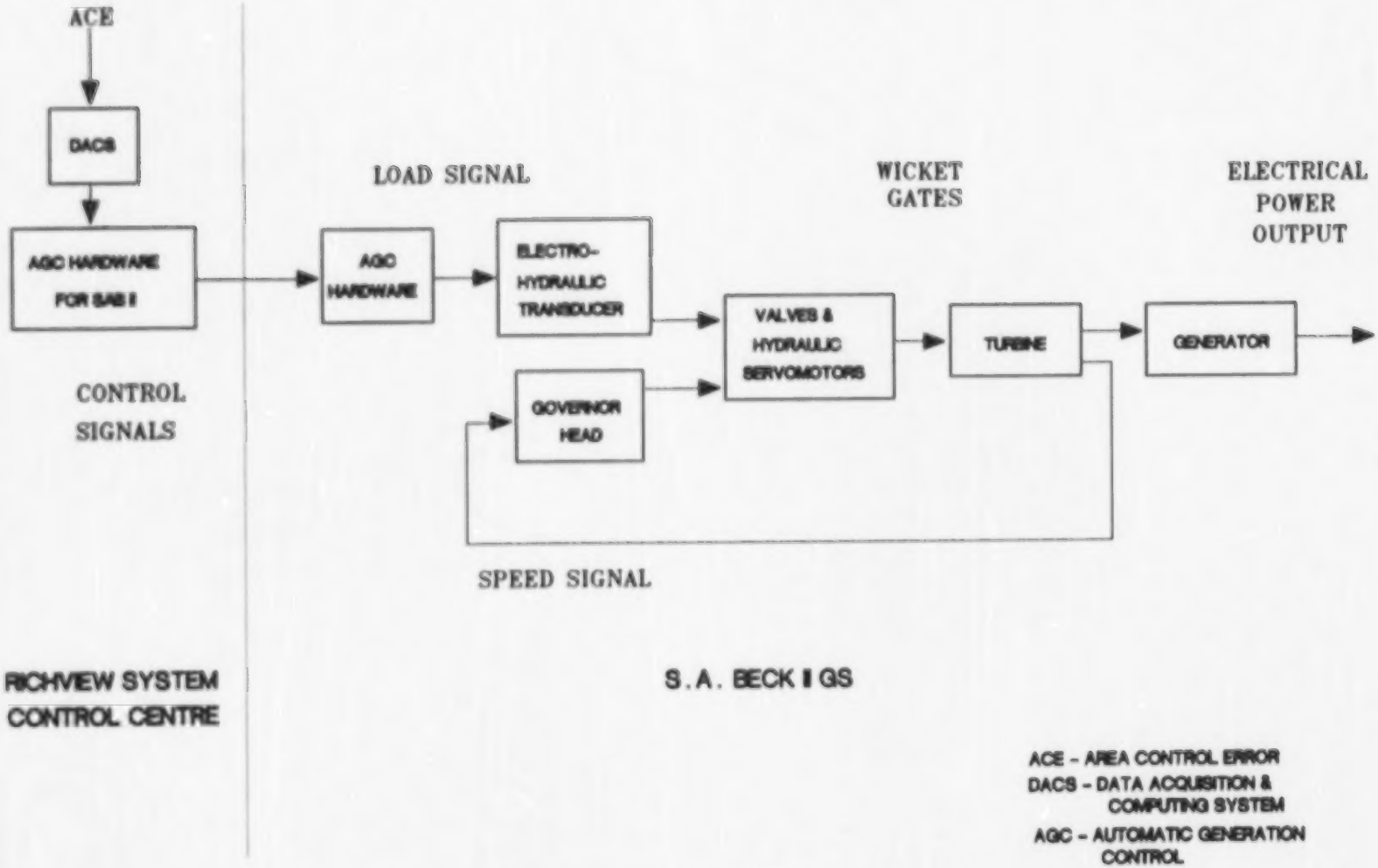

FIGURE 1

OVERVIEW OF AGC SYSTEM AT S.A. BECK II GS

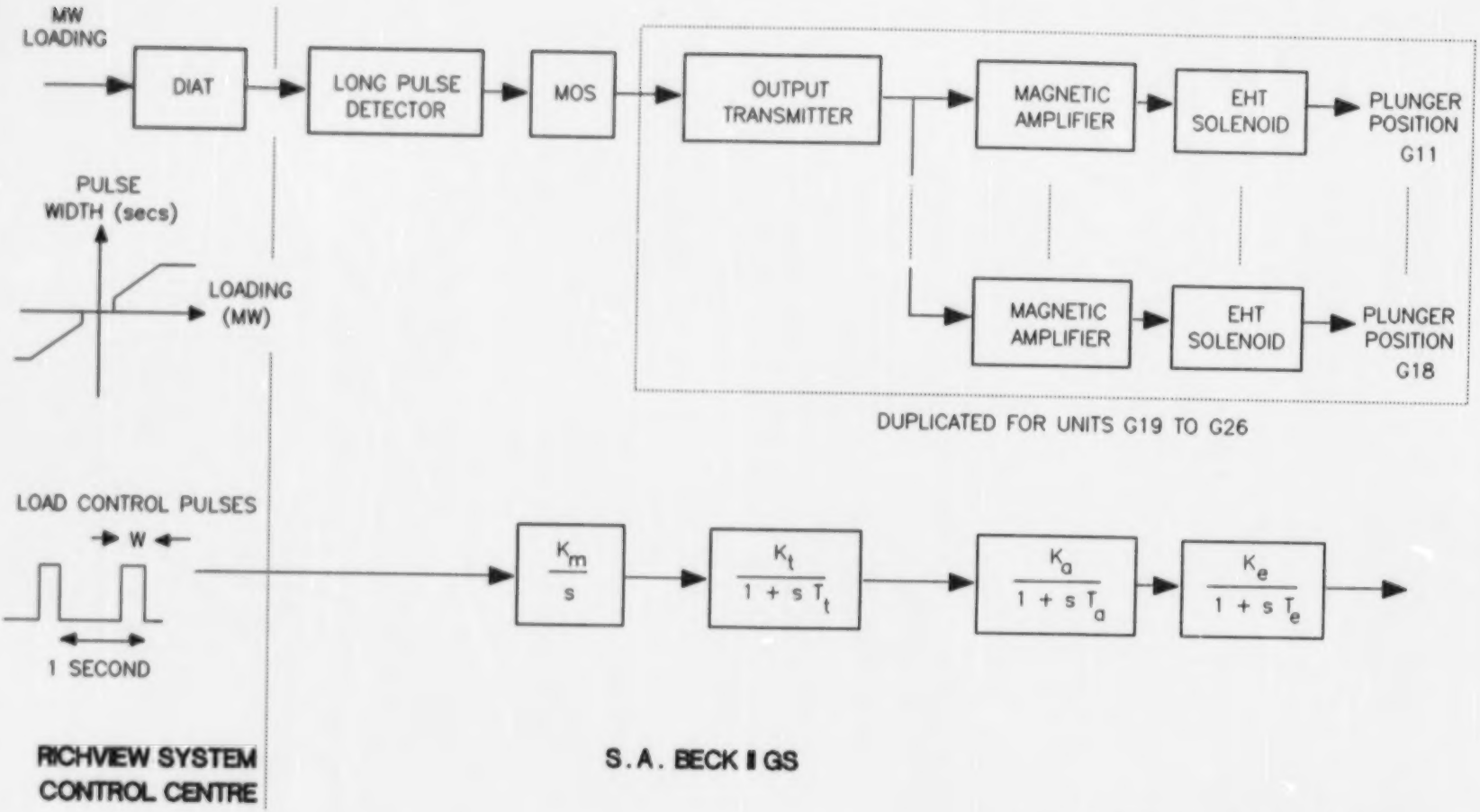

DIAT – DIRECTIONAL IMPULSE ADJUSTING TYPE CONTROL SYSTEM

MOS – MOTOR OPERATED SETTER

EHT – ELECTRO–HYDRAULIC TRANSDUCER

FIGURE 2
REPRESENTATION OF AGC HARDWARE

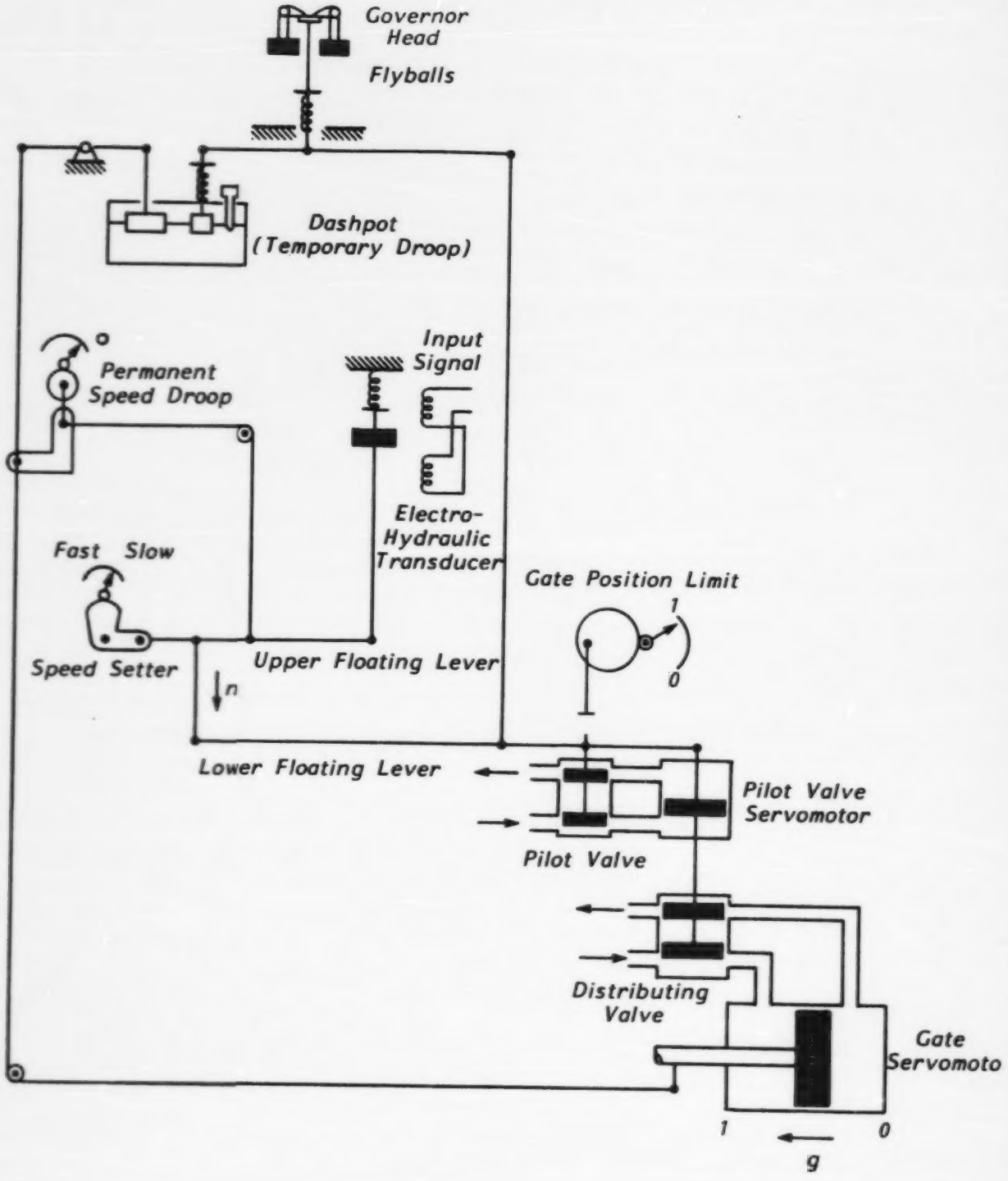

FIGURE 3

SCHEMATIC OF GOVERNOR WITH ELECTROHYDRAULIC TRANSDUCER

175247-RD

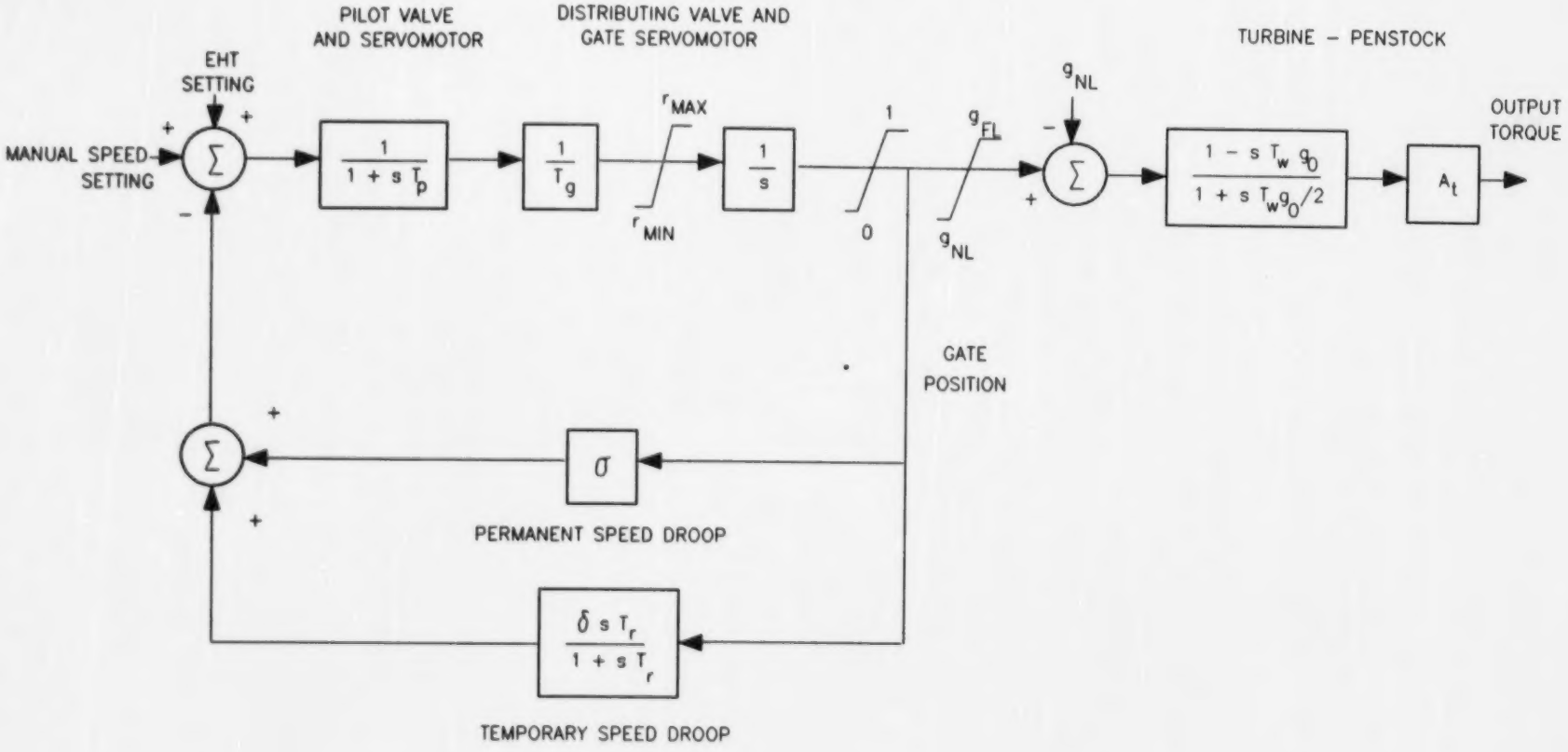

FIGURE 4

GOVERNOR – TURBINE TRANSFER FUNCTION BLOCK DIAGRAM

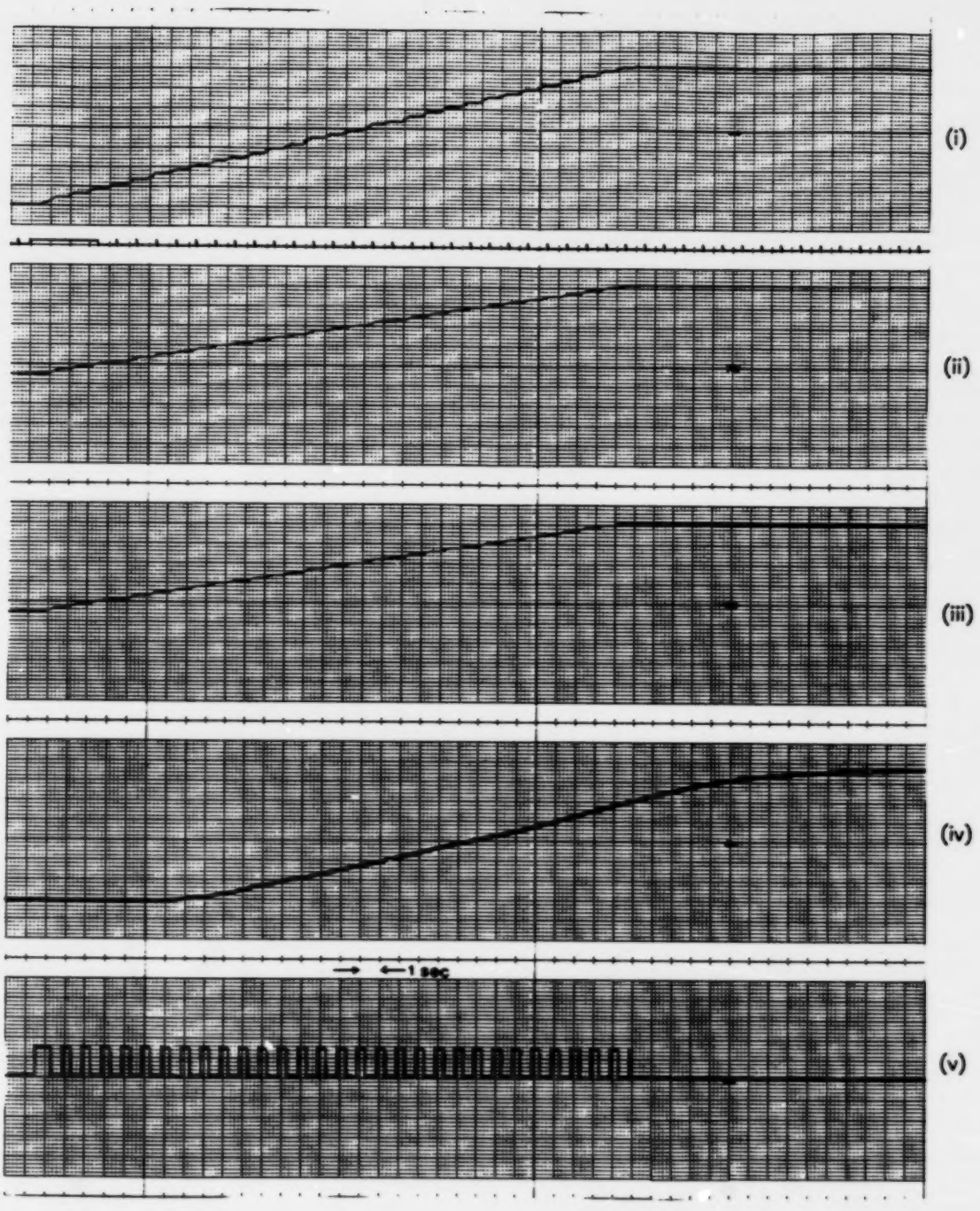

FIGURE 5 – AGC OPEN LOOP TEST (100%/MINUTE FOR 30 SECONDS)

(i) MOS OUTPUT (50 mV FS)
(ii) TRANSMITTER 1 OUTPUT (25 mA FS)
(iii) TRANSMITTER 2 OUTPUT (25 mA FS)
(iv) TOTAL PLANT OUTPUT (100 MW FS)
(v) RAISE PULSES

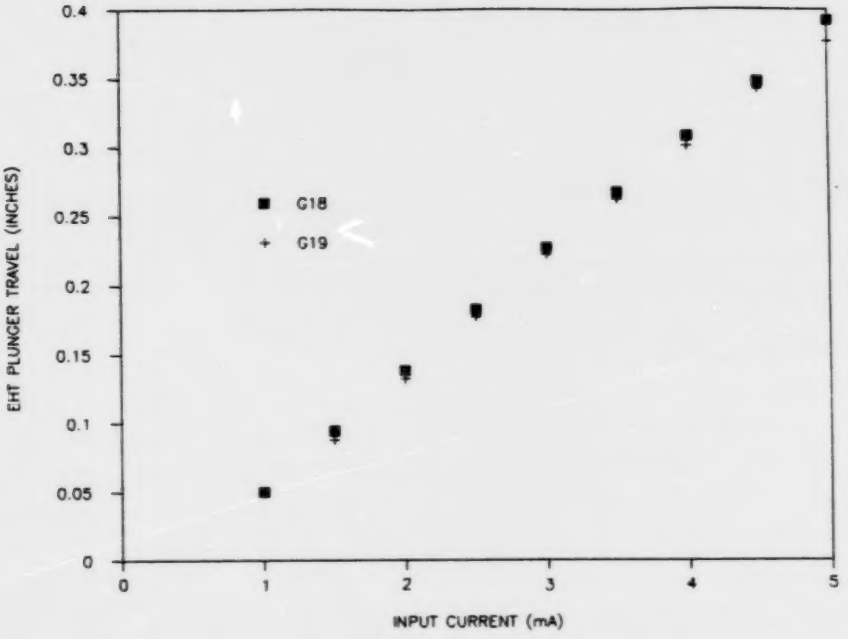

FIGURE 6 : ELECTRO-HYDRAULIC TRANSDUCER CALIBRATION CURVE

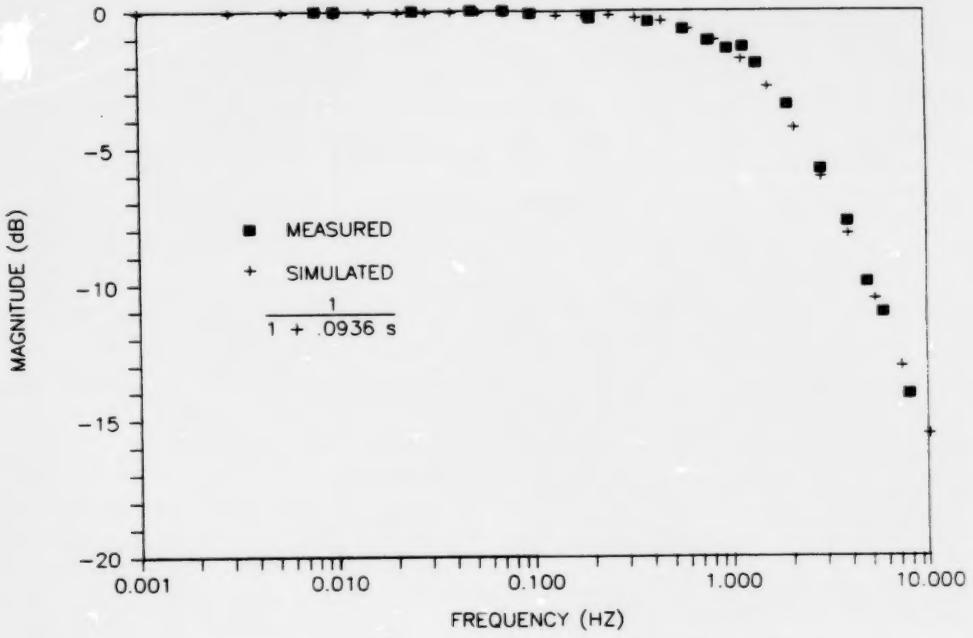

FIGURE 7(a) : MAGNETIC AMPLIFIER – MAGNITUDE RESPONSE

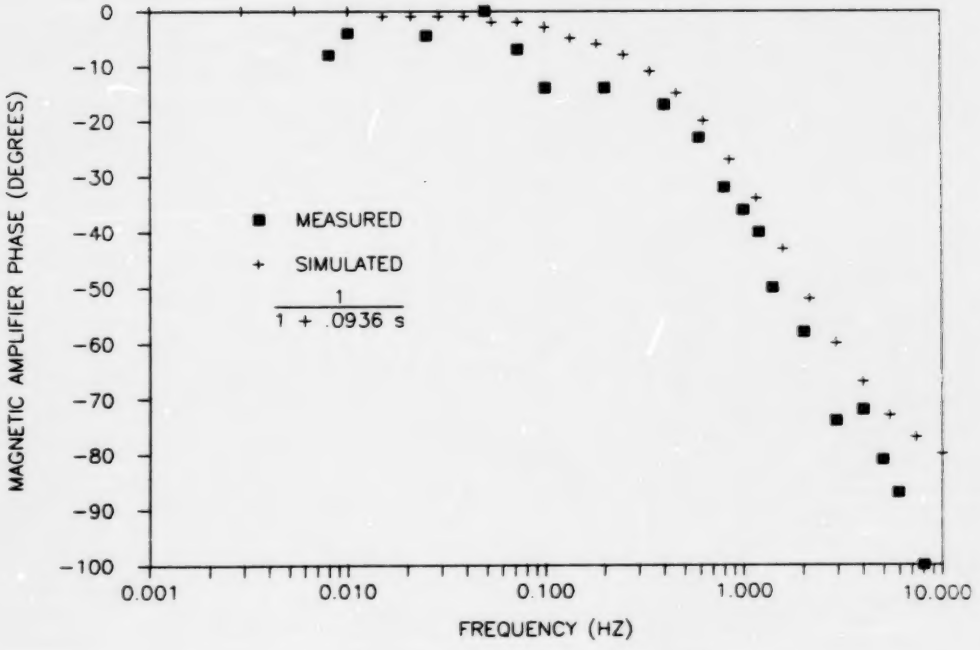

FIGURE 7(b) : MAGNETIC AMPLIFIER – PHASE RESPONSE

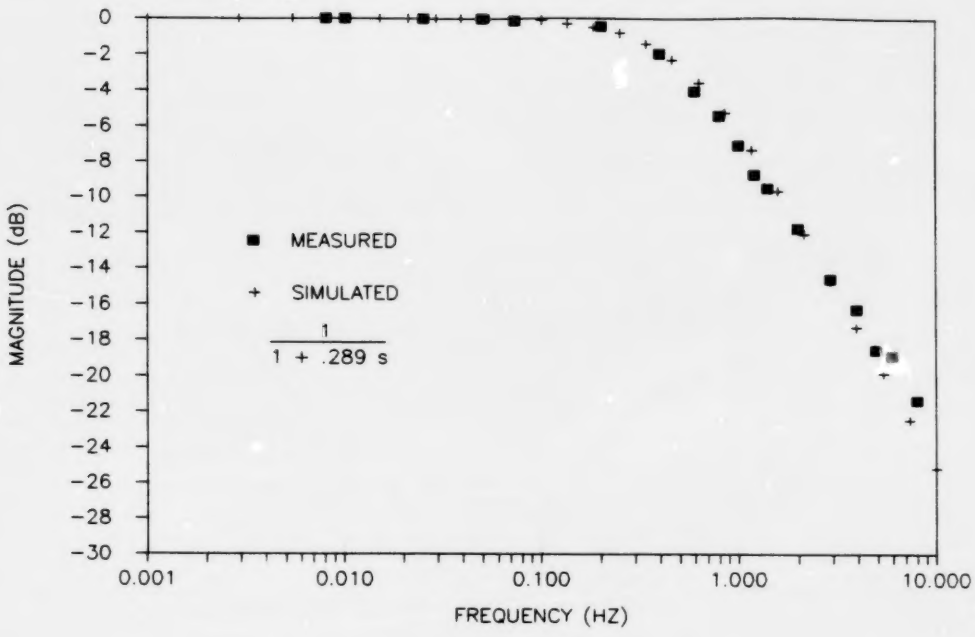

FIGURE 8(a) : EHT MAGNITUDE RESPONSE

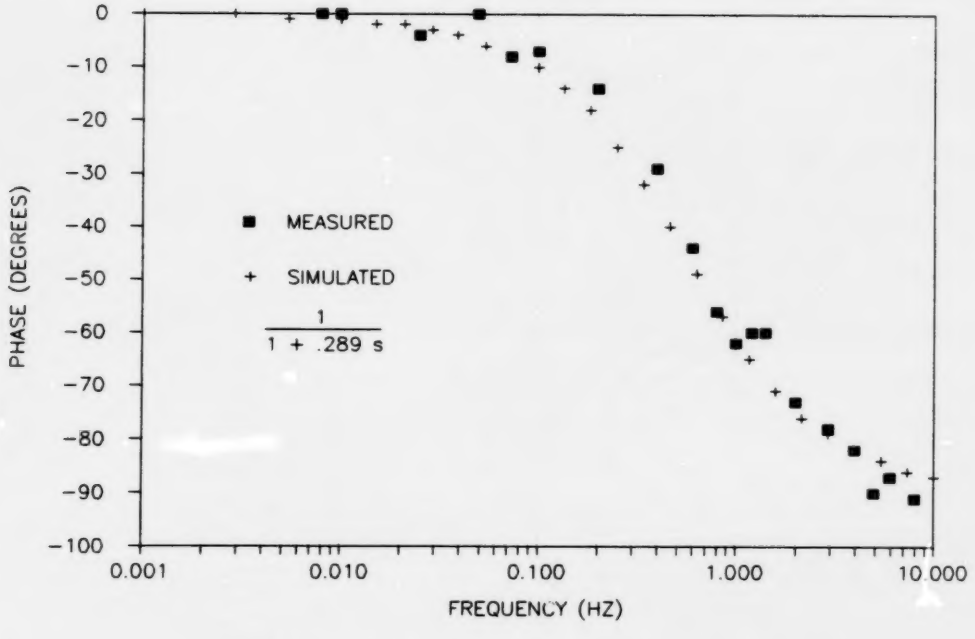

FIGURE 8(b) : EHT PHASE RESPONSE

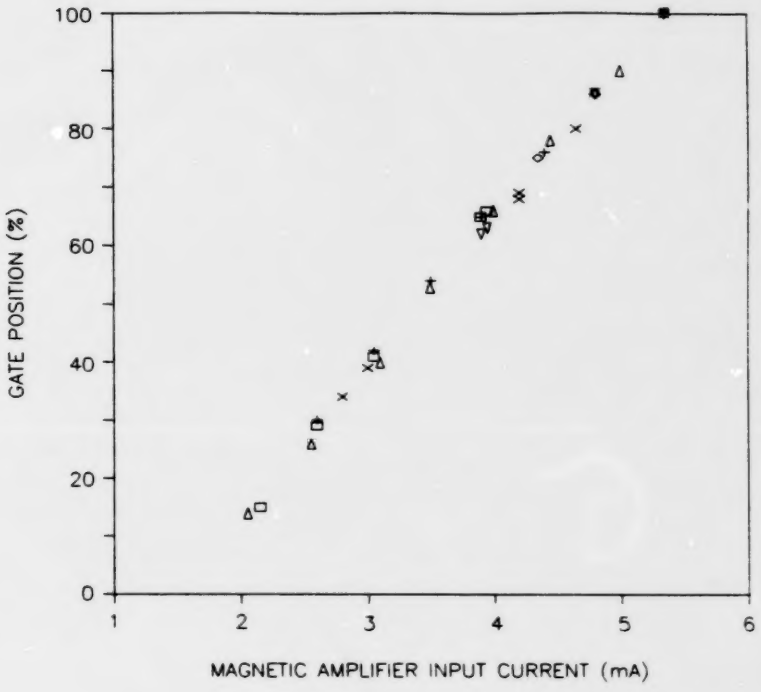

LEGEND : .5 mA DECREASING INPUT STEPS : □ TEST 1
△ TEST 2

.5 mA INCREASING INPUT STEPS : + TEST 1
○ TEST 2

1 TO 2.5 mA INCREASING AND DECREASING INPUT STEPS : ▽ TEST 1
× TEST 2

FIGURE 9 : STEADY STATE GATE POSITION FOLLOWING MAGNETIC AMPLIFIER STEP INPUT TESTS

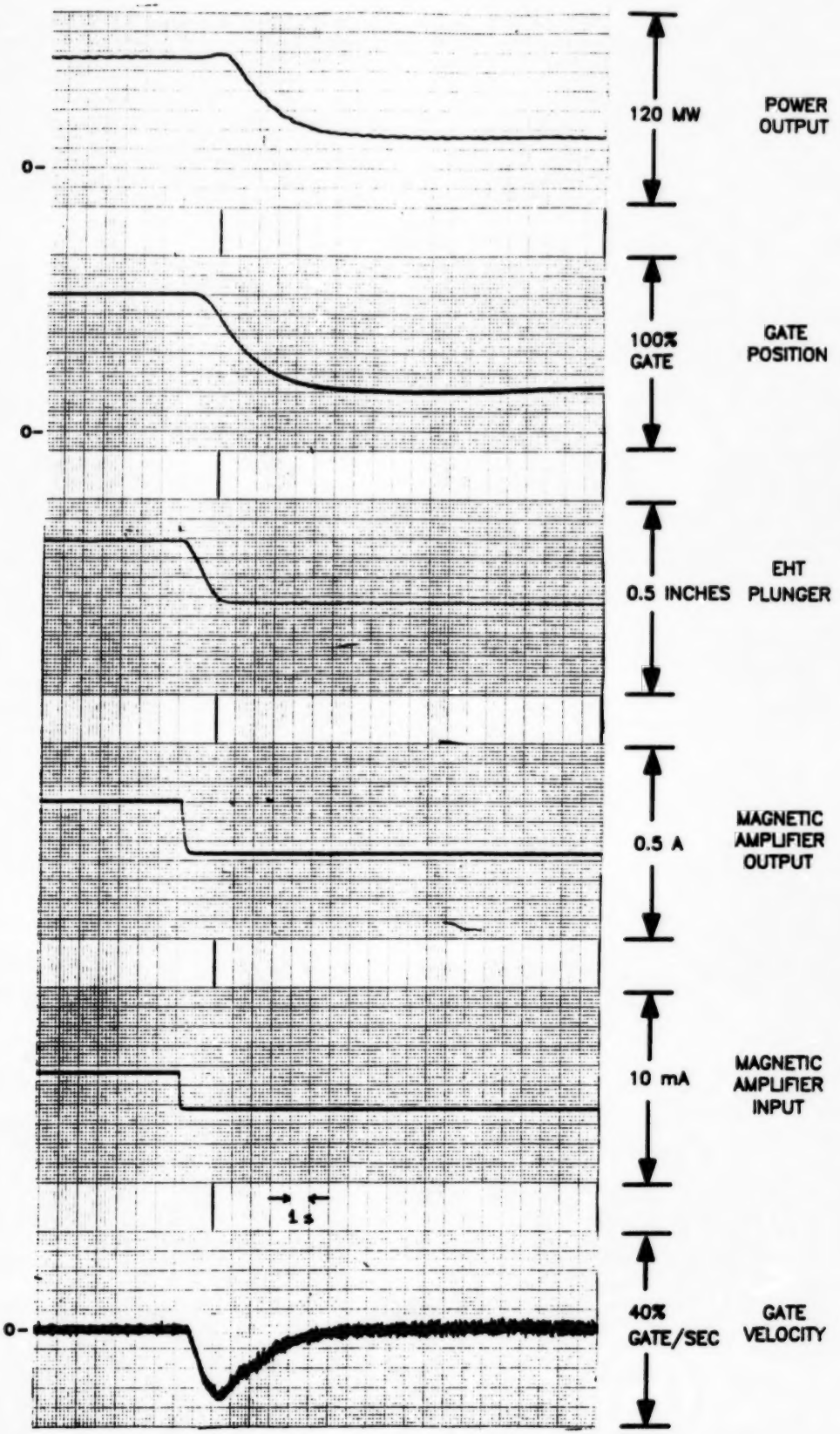

FIGURE 10 : MEASURED STEP TEST RESULTS – CLOSING STEP (1 sec / large div)

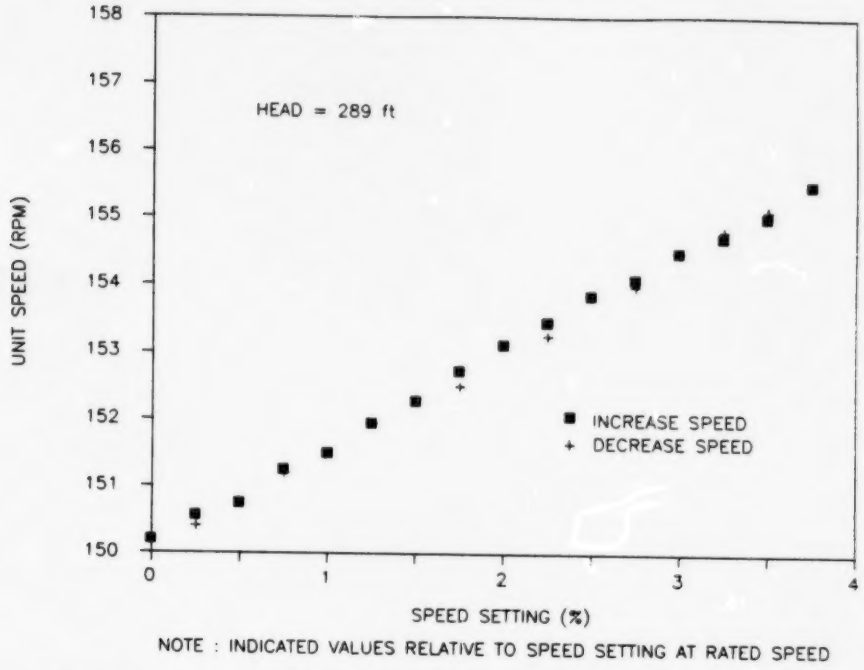

FIGURE 11 : SPEED SETTER CALIBRATION (UNIT G19)

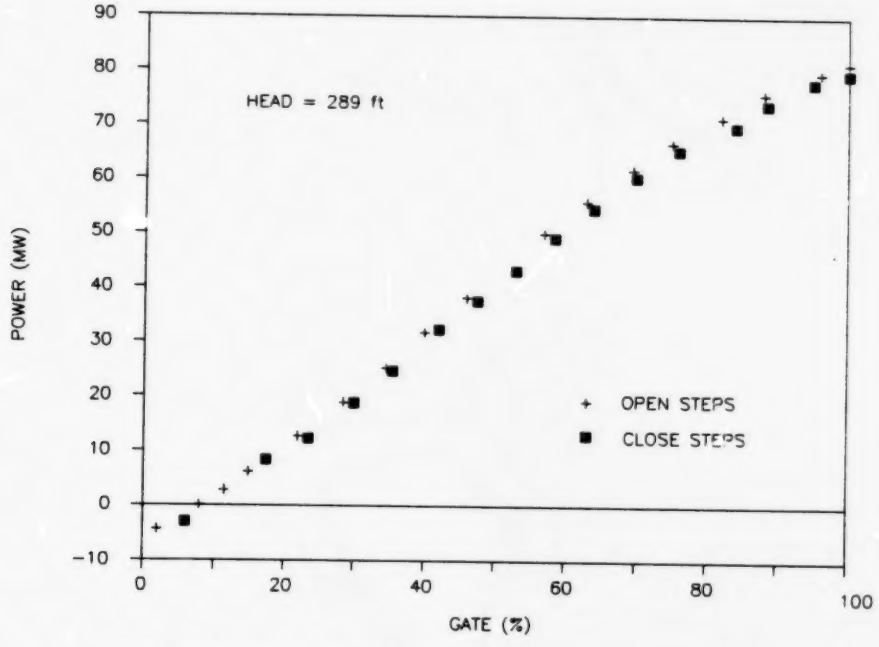

FIGURE 12 : POWER VS. GATE (UNIT G19)

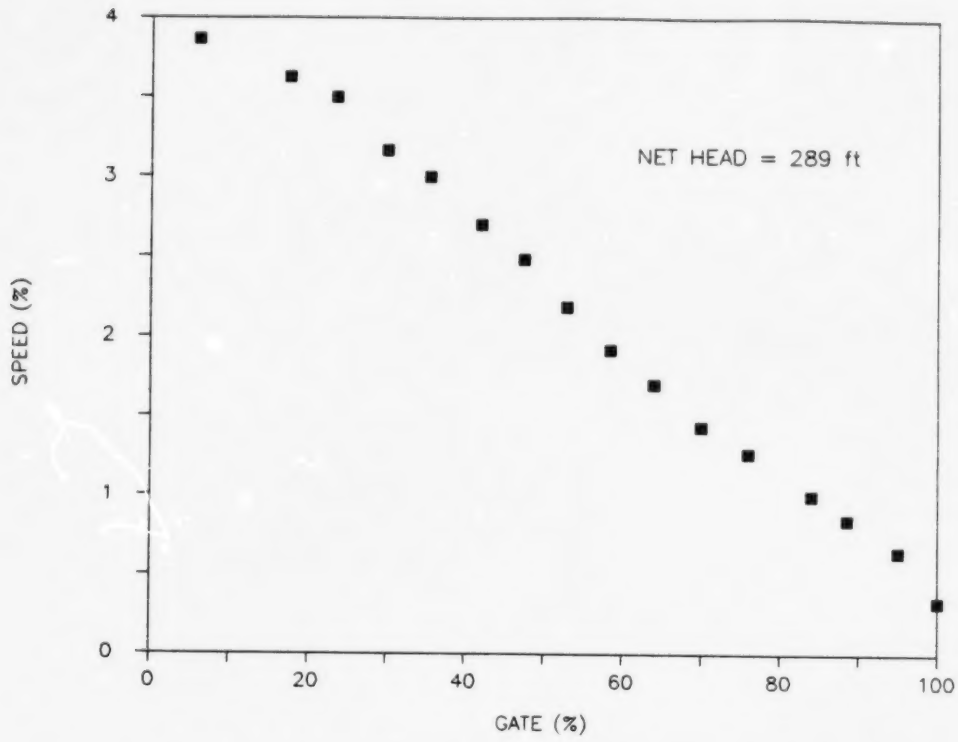

FIGURE 13 : INCREMENTAL PERMANENT SPEED DROOP

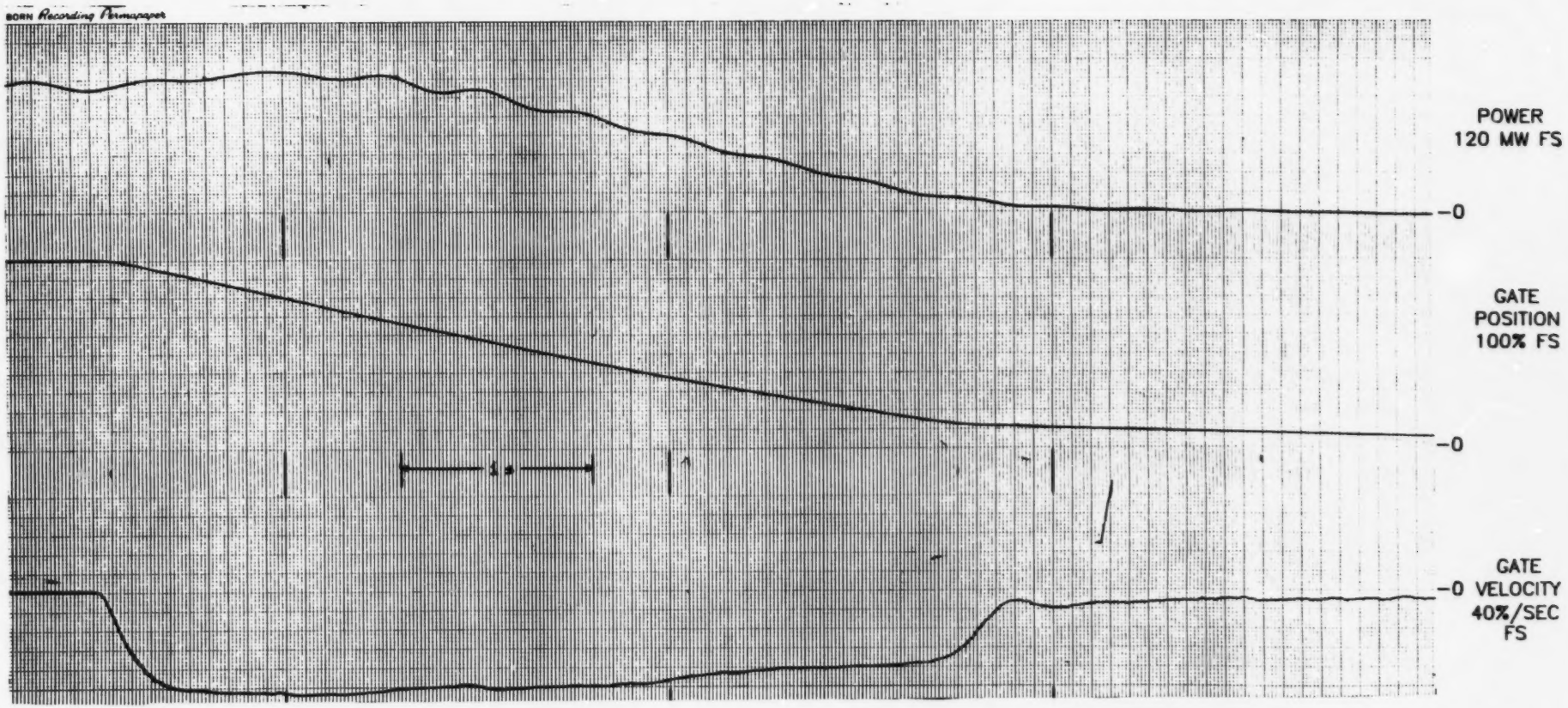

FIGURE 14 – GATE LIMIT CLOSING STEP

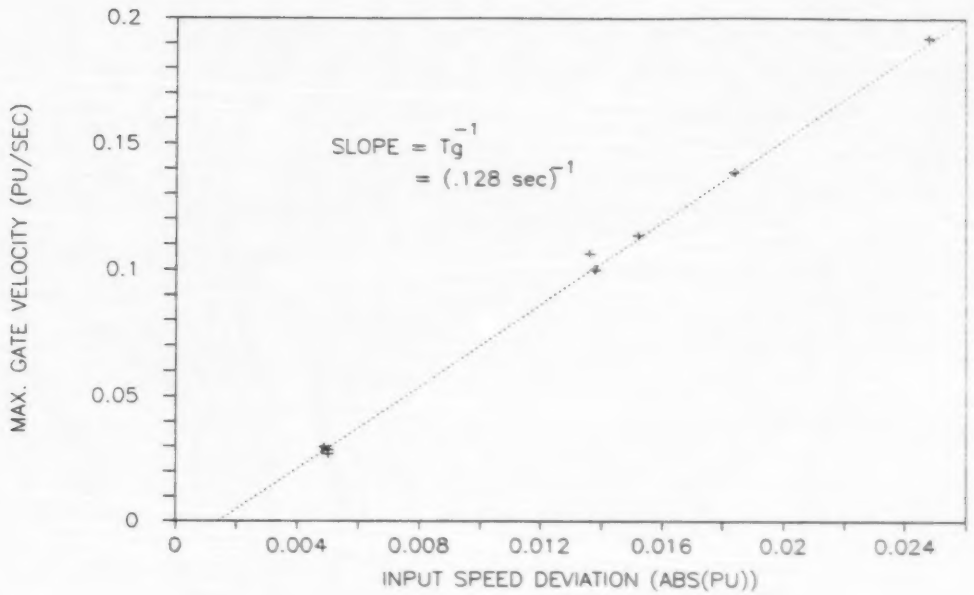

FIGURE 15(a) : DETERMINATION OF Tg – GATE CLOSING STEPS

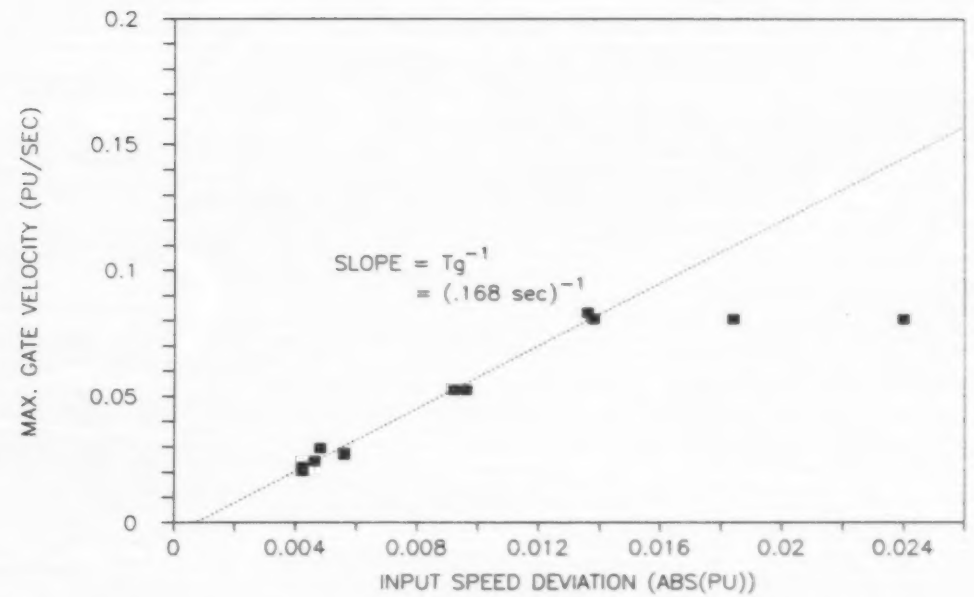

FIGURE 15(b) : DETERMINATION OF Tg – GATE OPENING STEPS

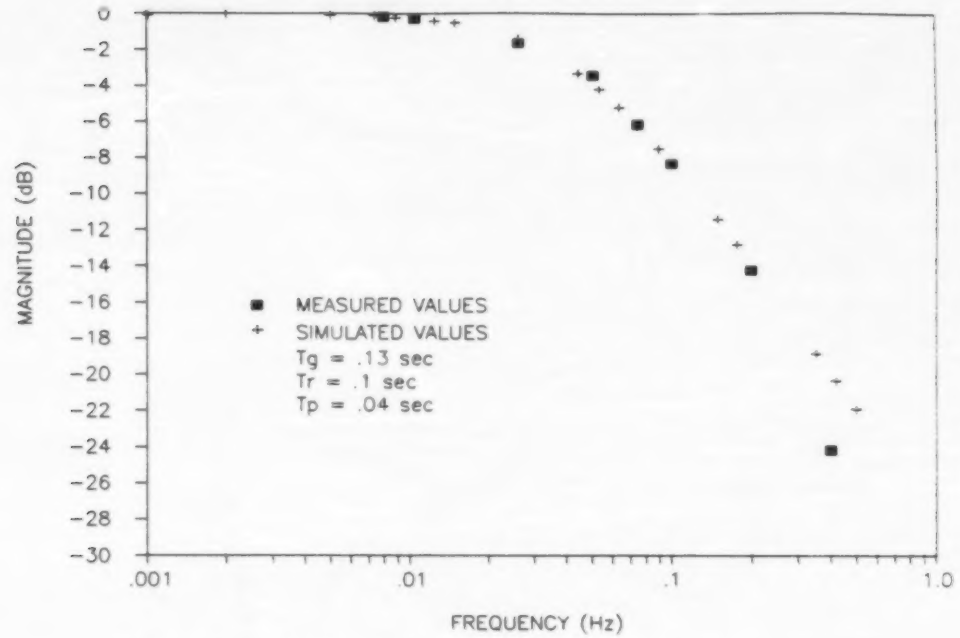

FIGURE 16(a) : GATE FREQUENCY RESPONSE – MAGNITUDE

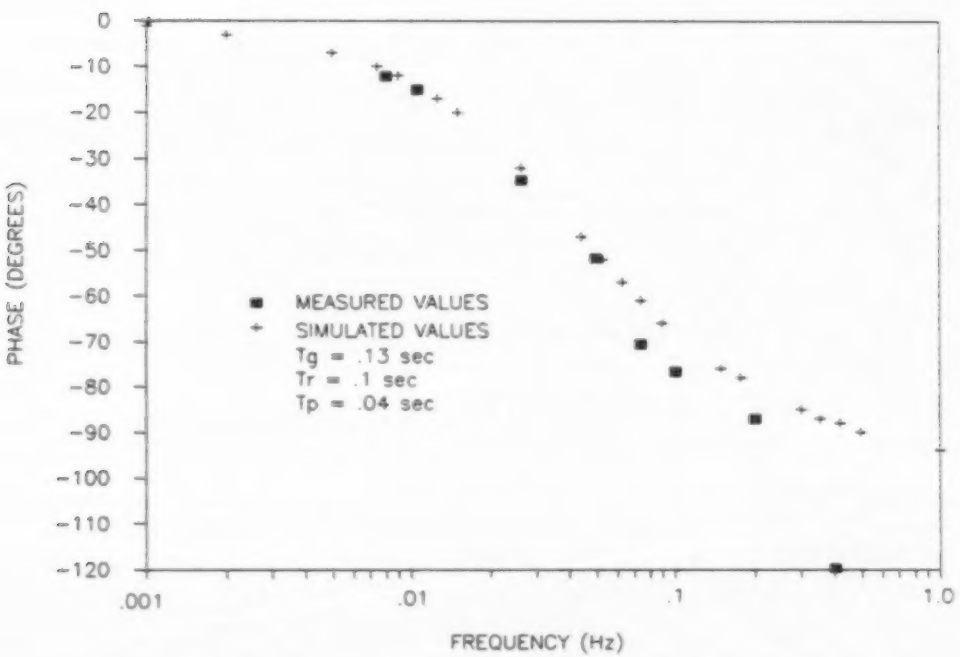

FIGURE 16(b) : GATE FREQUENCY RESPONSE – PHASE

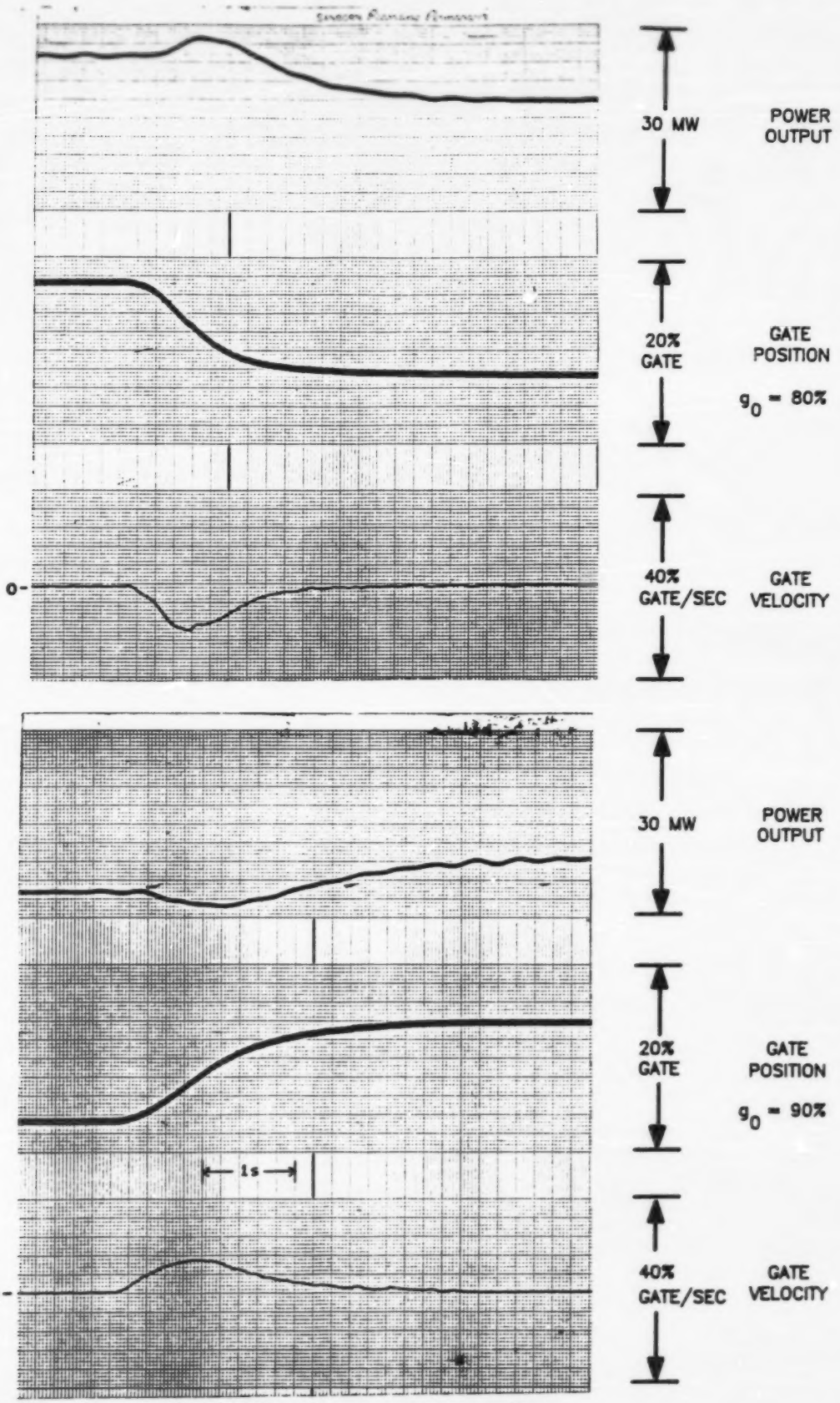

FIGURE 17 : 10% GATE LIMIT STEP TESTS
UPPER – GATE CLOSING STEP
LOWER – GATE OPENING STEP

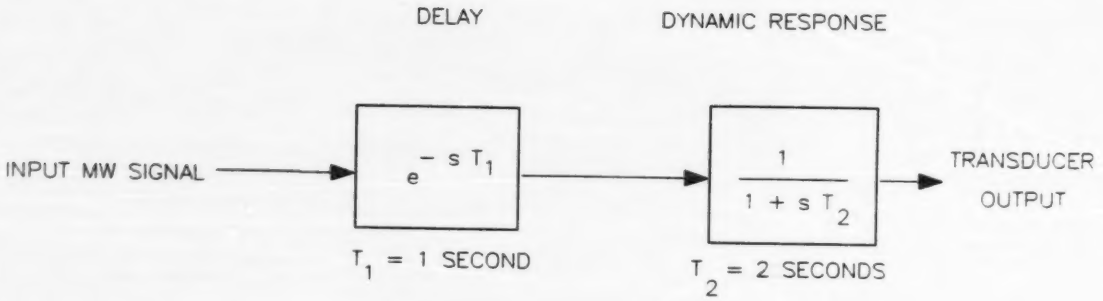

(a) SANGAMO AW6S WATT TRANSDUCER

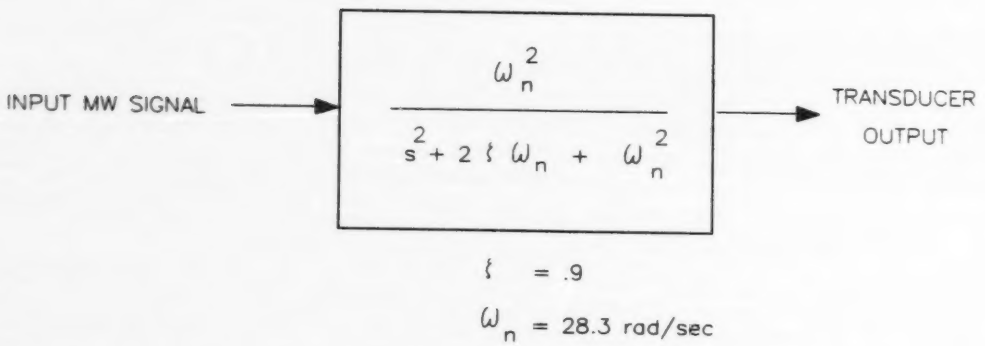

(b) SCIENTIFIC COLUMBUS XL31K5A2–OH WATT TRANSDUCER

FIGURE 18 : WATT TRANSDUCER TRANSFER FUNCTION BLOCK DIAGRAMS

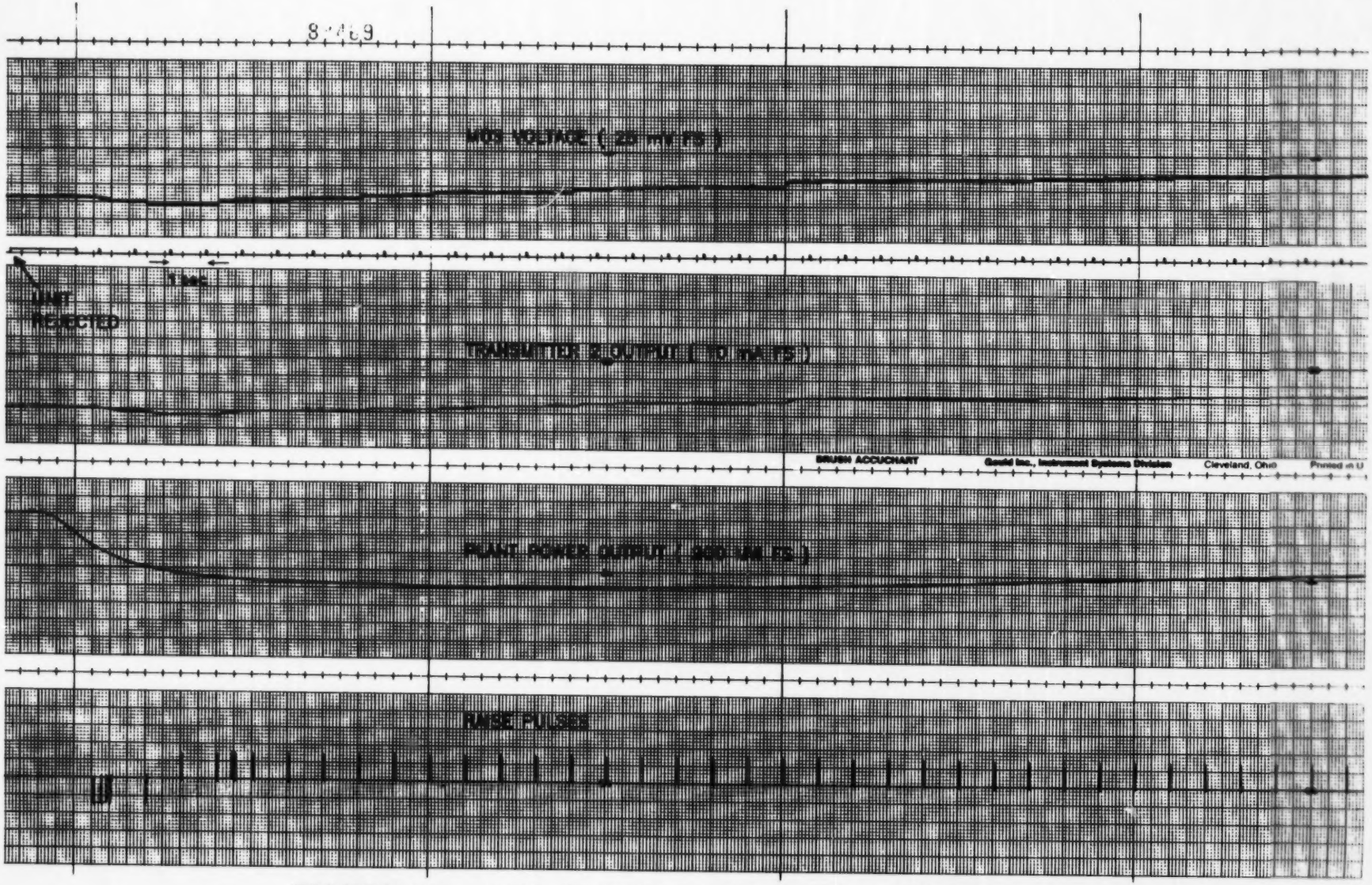

FIGURE 19 : AGC CLOSED LOOP TEST – UNIT REJECTION

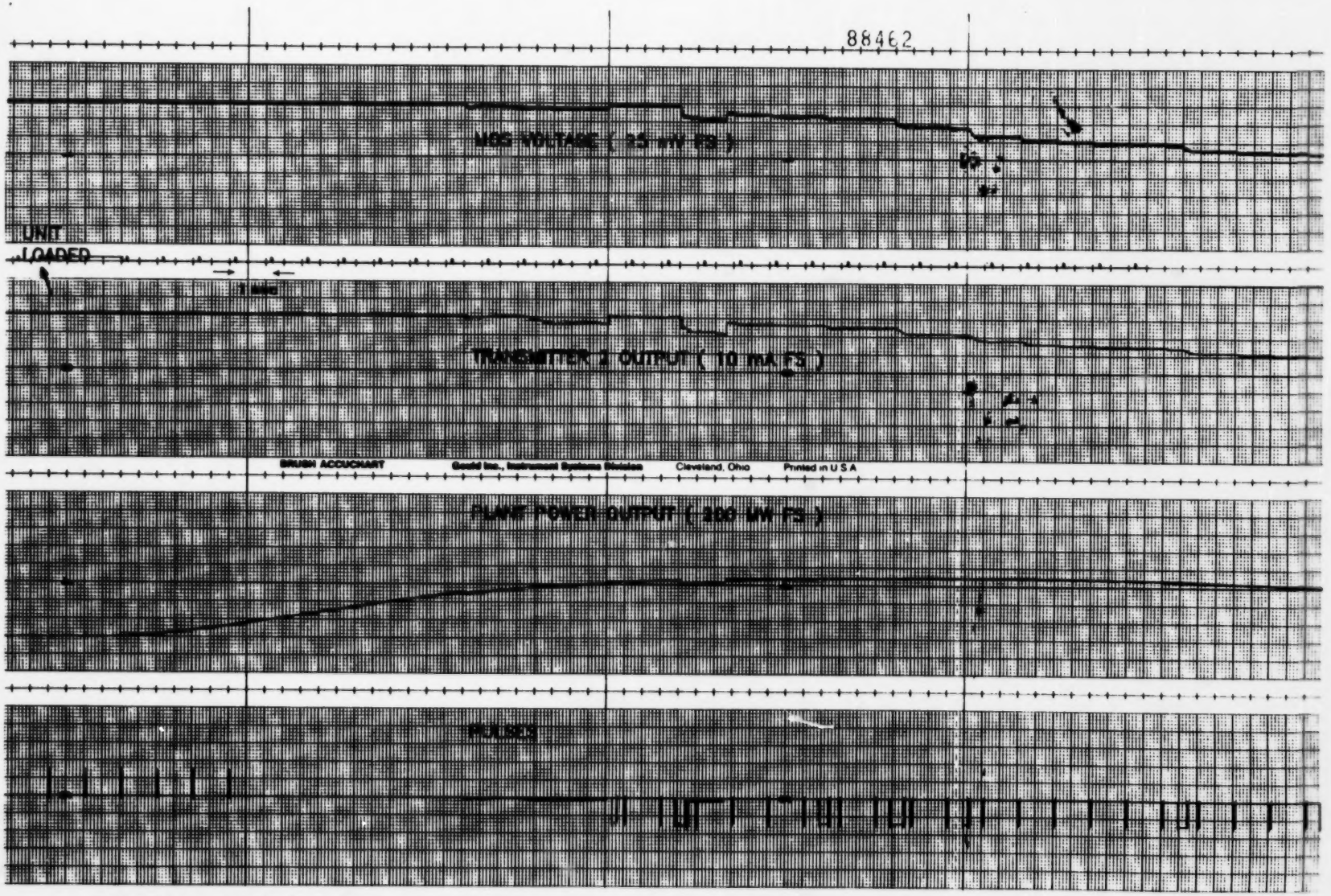

FIGURE 20(a) : AGC CLOSED LOOP TEST – RAPID LOADING (CONTINUED)

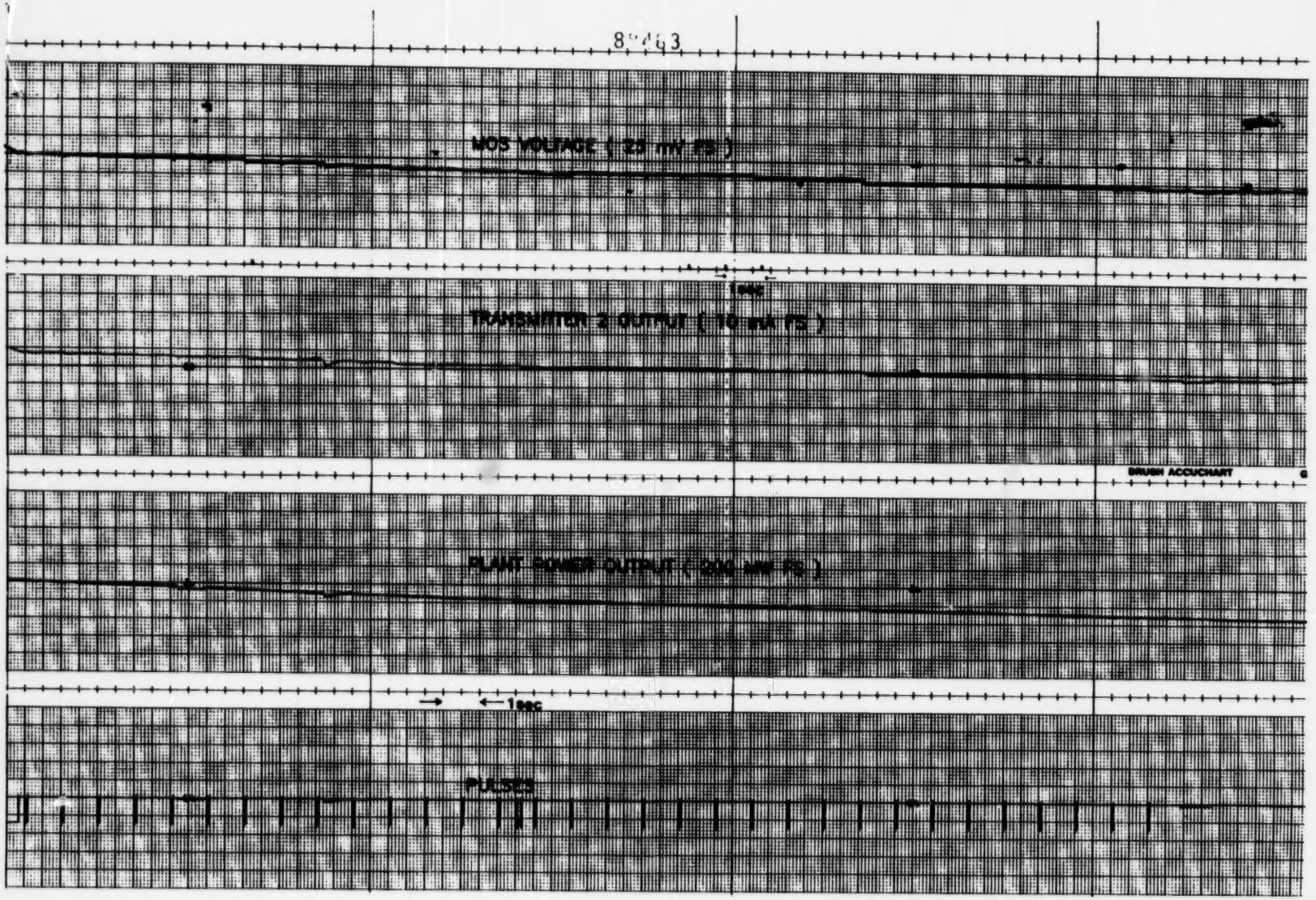

FIGURE 20(b) CONT'D: AGC CLOSED LOOP TEST – RAPID LOADING

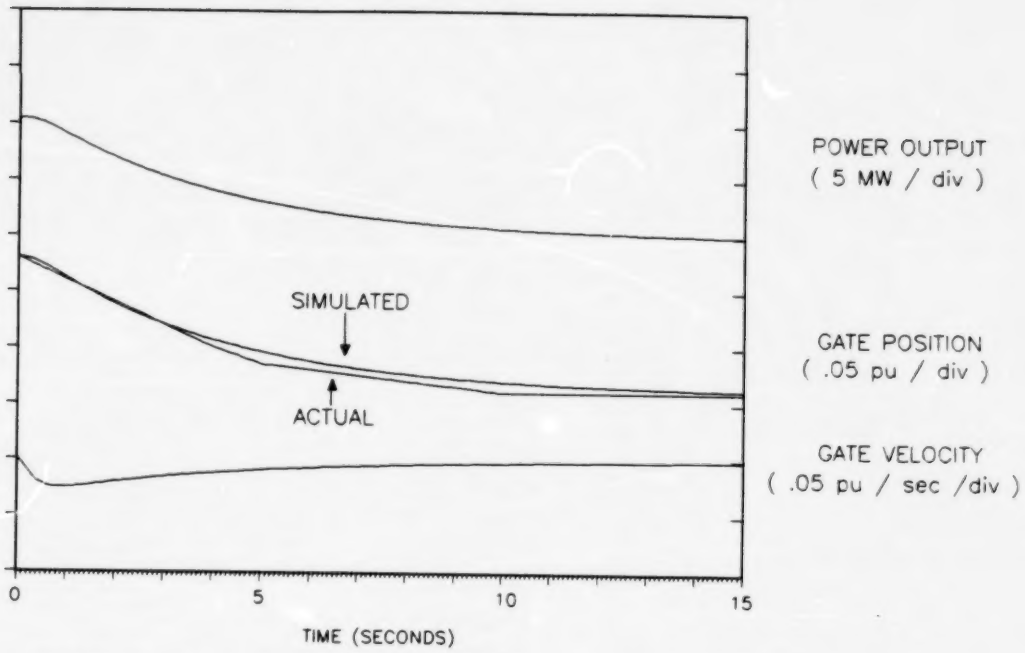

FIGURE 21 : SIMULATED MAGNETIC AMPLIFIER STEP TEST

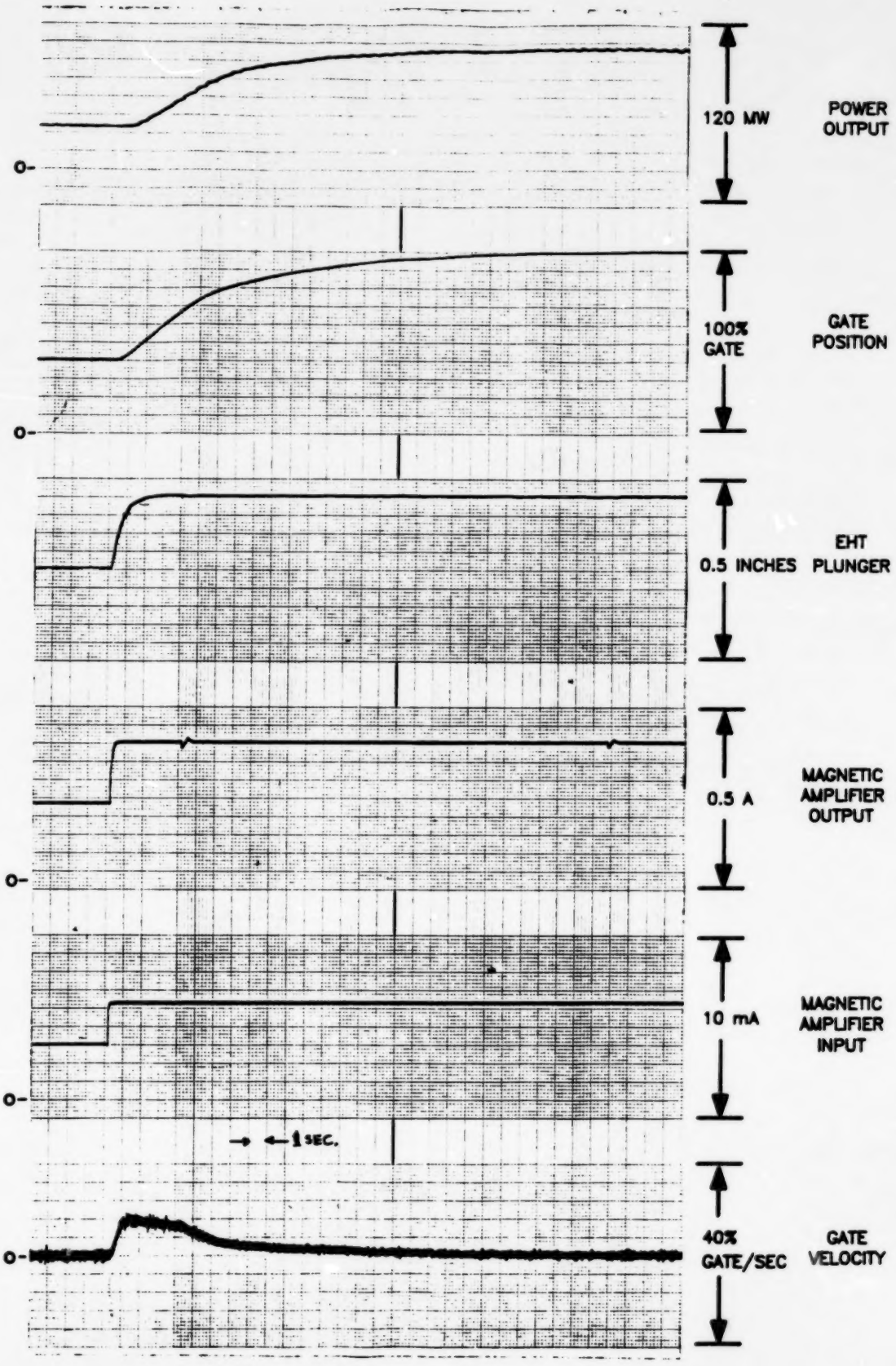

FIGURE 22 (a) : MEASURED STEP TEST RESULTS – OPENING STEP

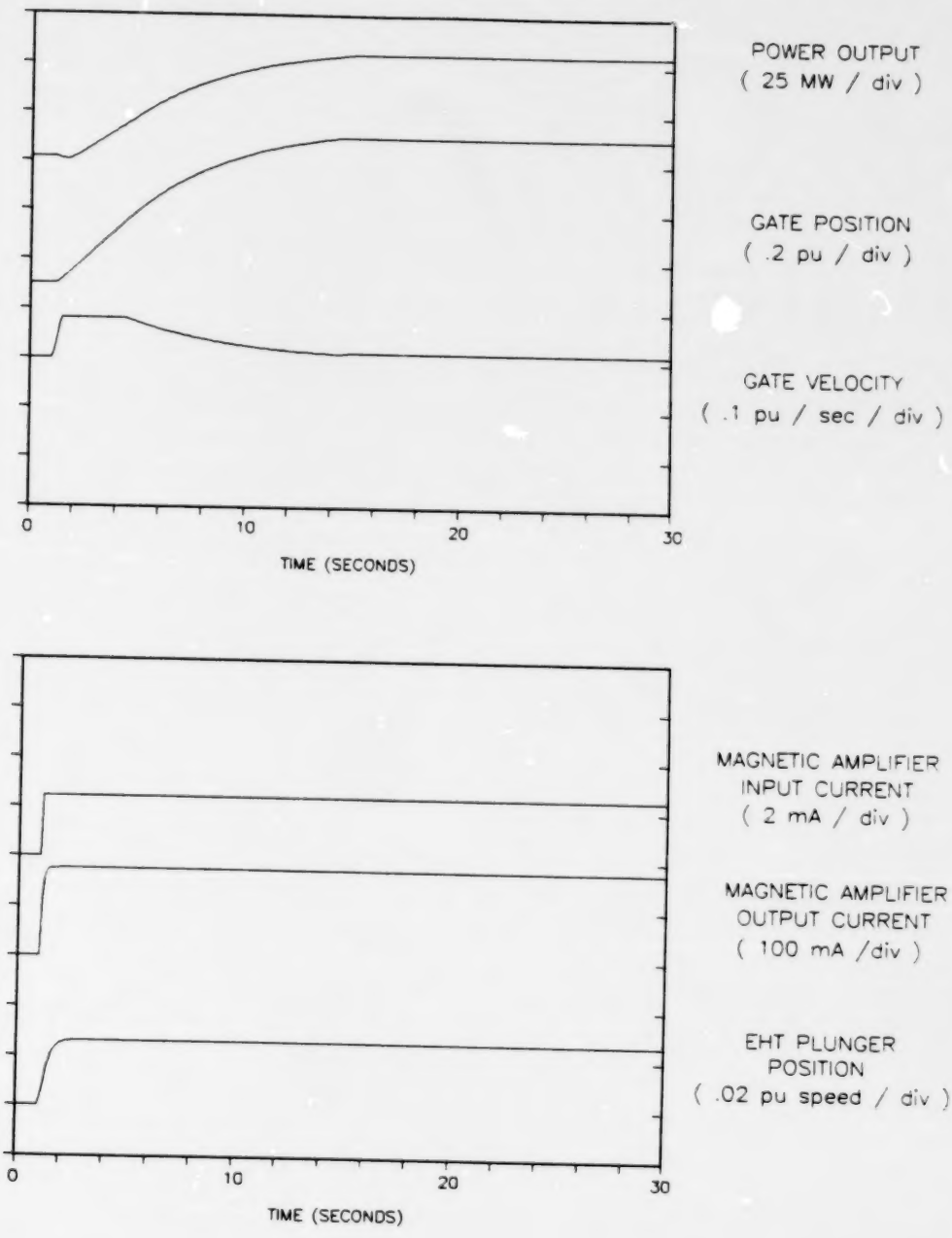

FIGURE 22 (b) : SIMULATED MAGNETIC AMPLIFIER STEP TEST

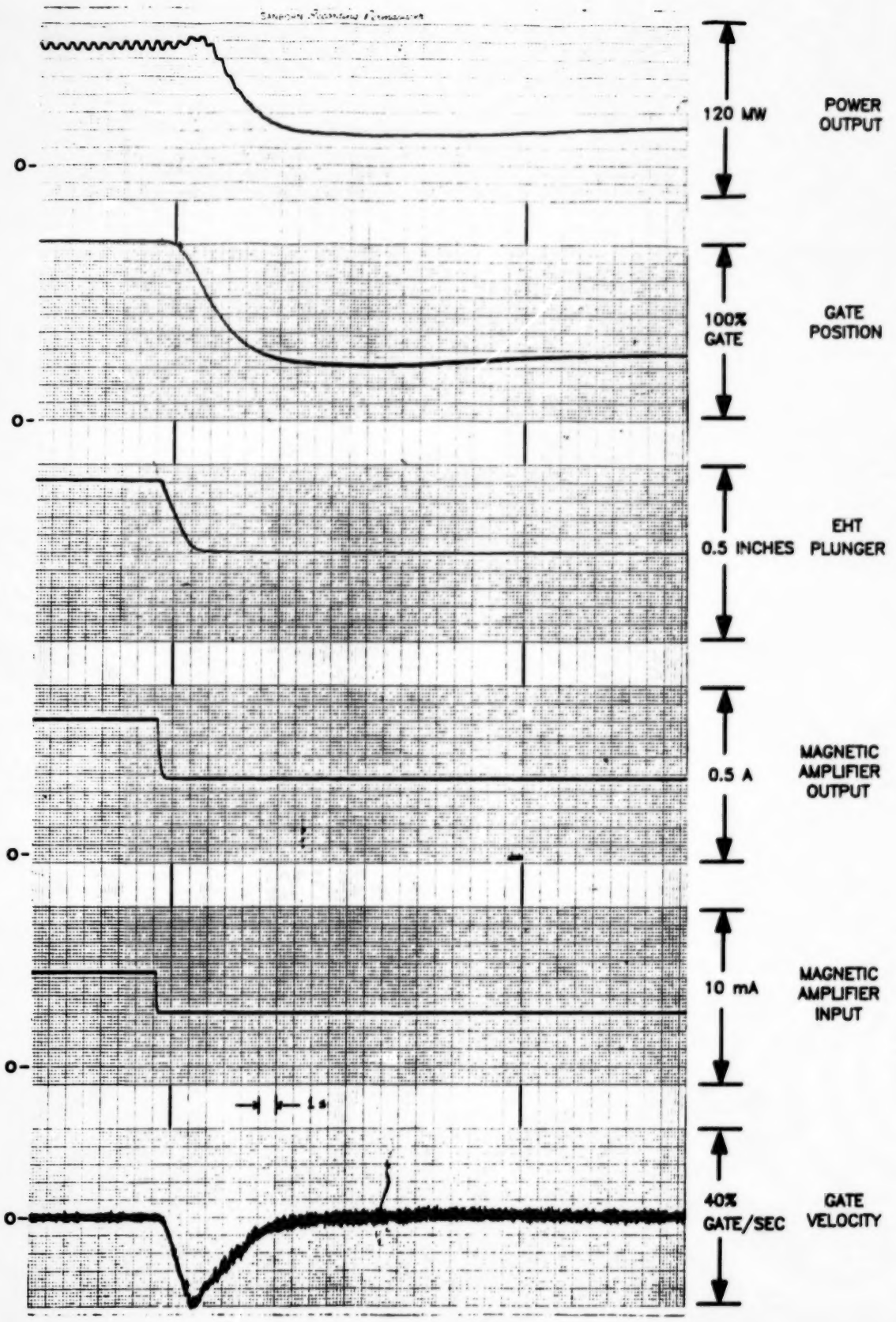

FIGURE 23(a) : MEASURED STEP TEST RESULTS – LARGE CLOSING STEP

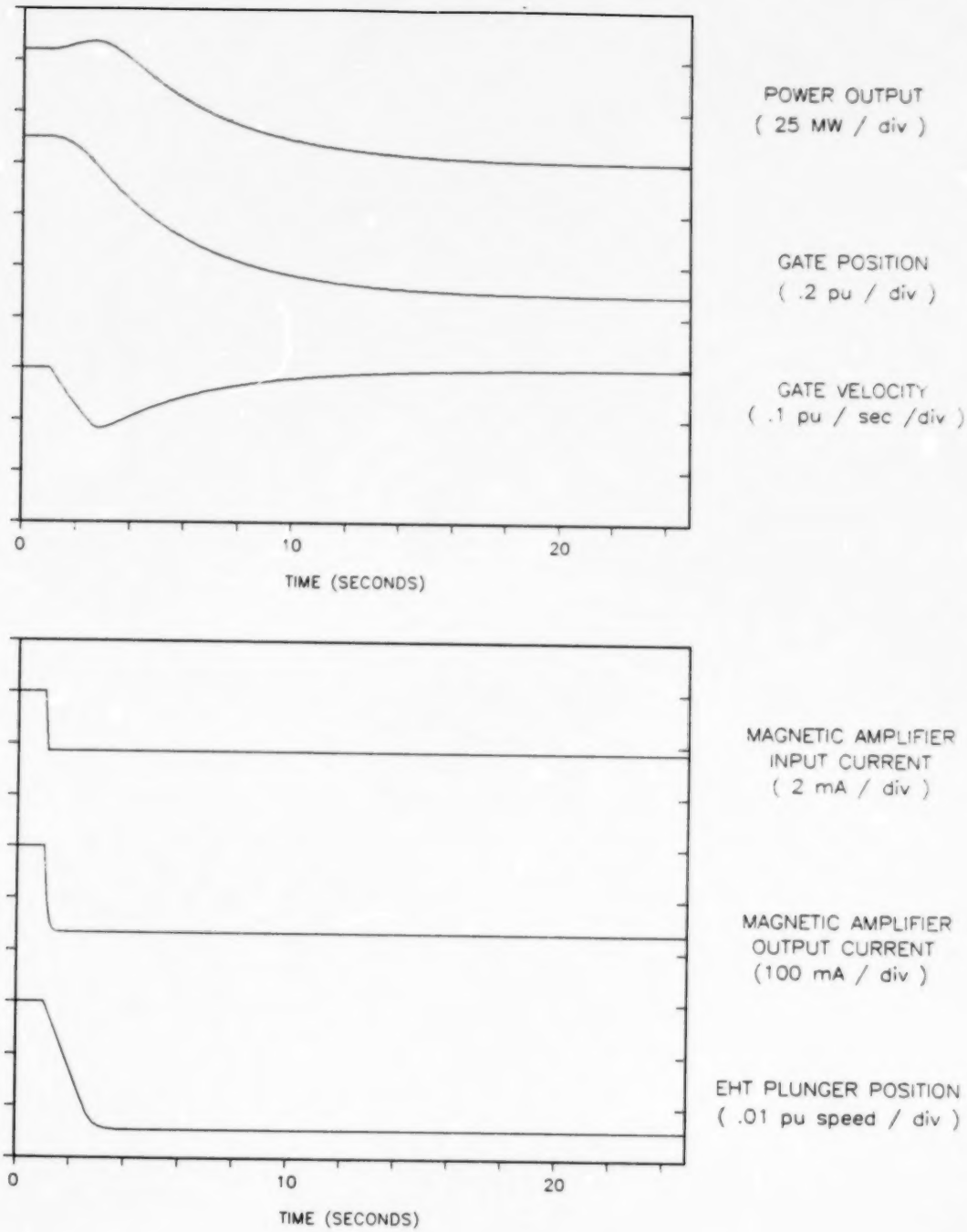

FIGURE 23 (b) : SIMULATED STEP TEST RESULTS
GATE CLOSING DIRECTION

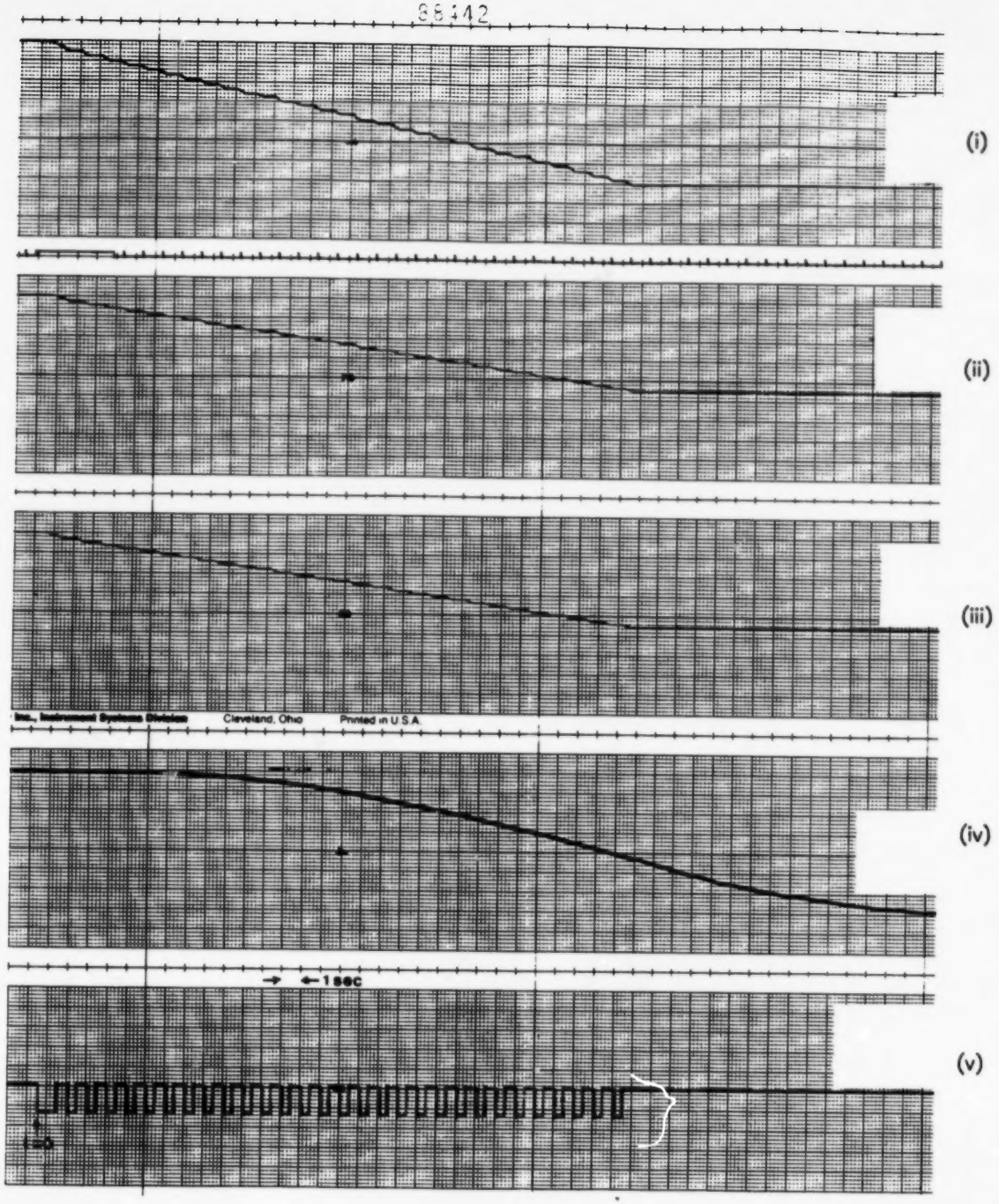

FIGURE 24(a):AGC OPEN LOOP TEST (−100%/MINUTE FOR 30 SECONDS)

(i) MOS OUTPUT (50 mV FS)
(ii) TRANSMITTER 1 OUTPUT (25 mA FS)
(iii) TRANSMITTER 2 OUTPUT (25 mA FS)
(iv) TOTAL PLANT OUTPUT (100 MW FS)
(v) LOWER PULSES
TIME SCALE = 1 SECOND/MAJOR DIVISION

CONTINUED NEXT PAGE

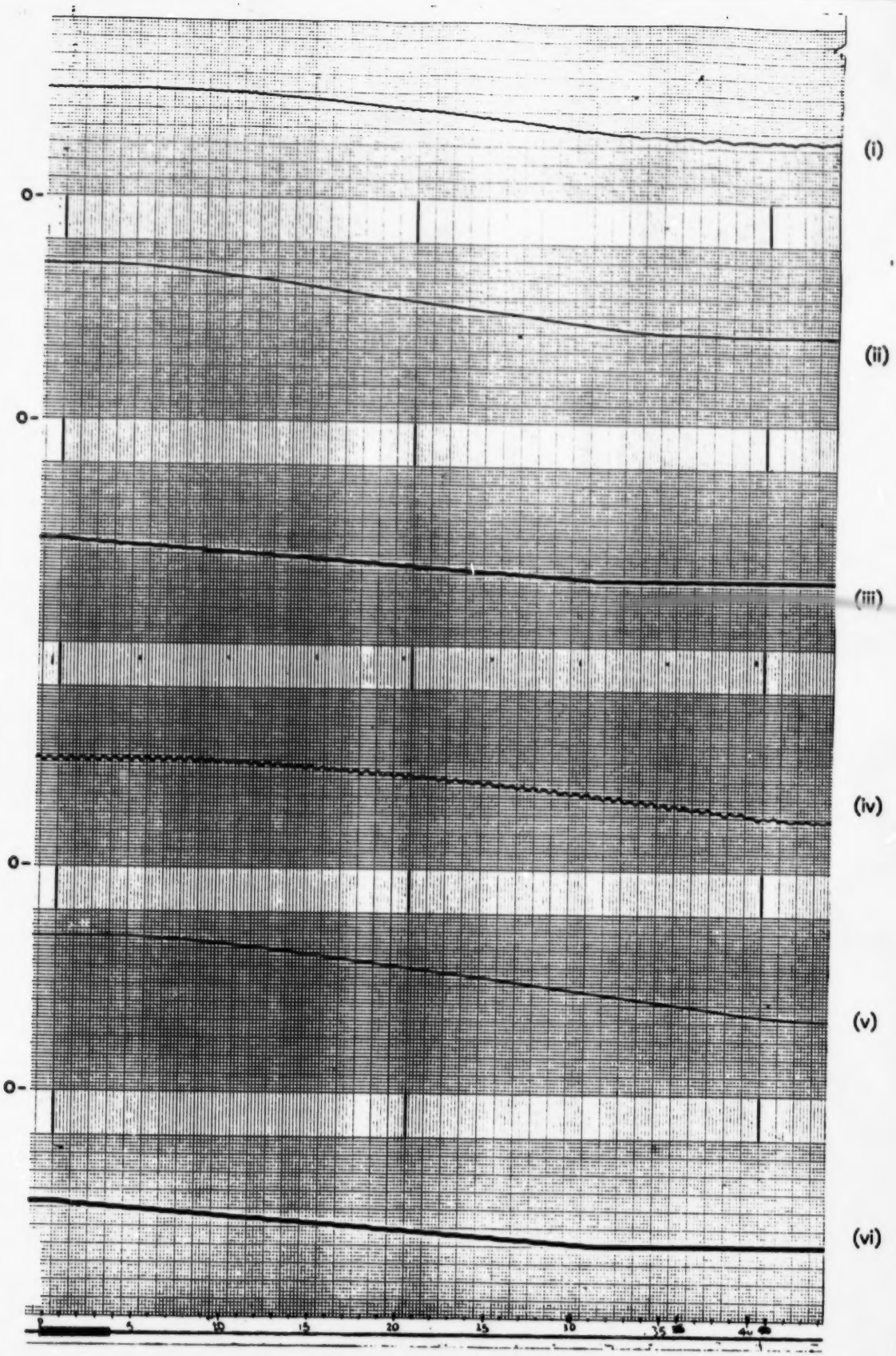

FIGURE 24(b):AGC OPEN LOOP TEST (CONT'D)

(i) & (iv) : G19 & G18 POWER OUTPUT (120 MW FS)
(ii) & (v) : G19 & G18 GATE POSITION (100% GATE FS)
(iii) & (vi) : G19 & G18 MAGNETIC AMPLIFIER OUTPUT (.5 A FS)

CONTINUED NEXT PAGE

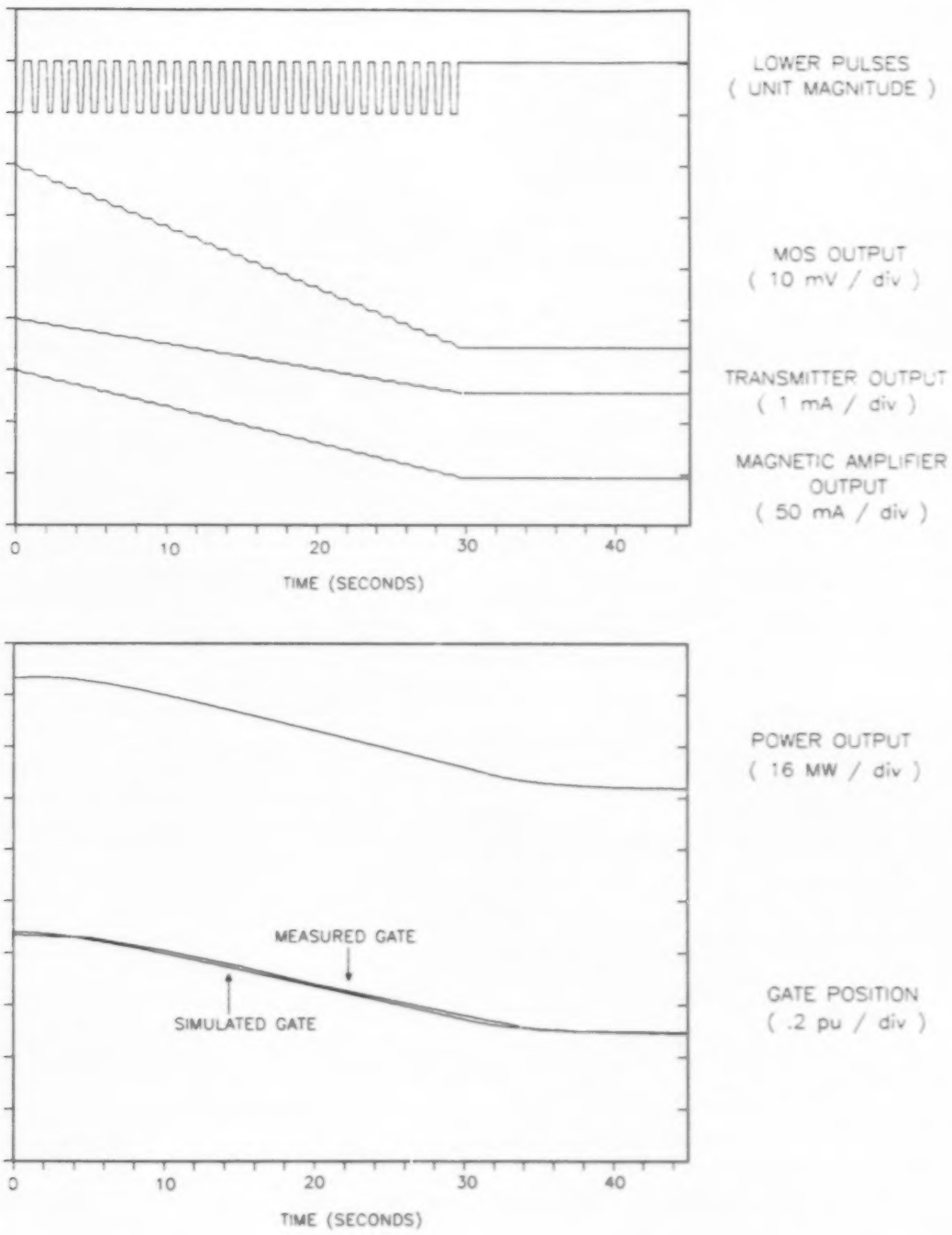

FIGURE 24 (c) : SIMULATED AGC OPEN LOOP TEST

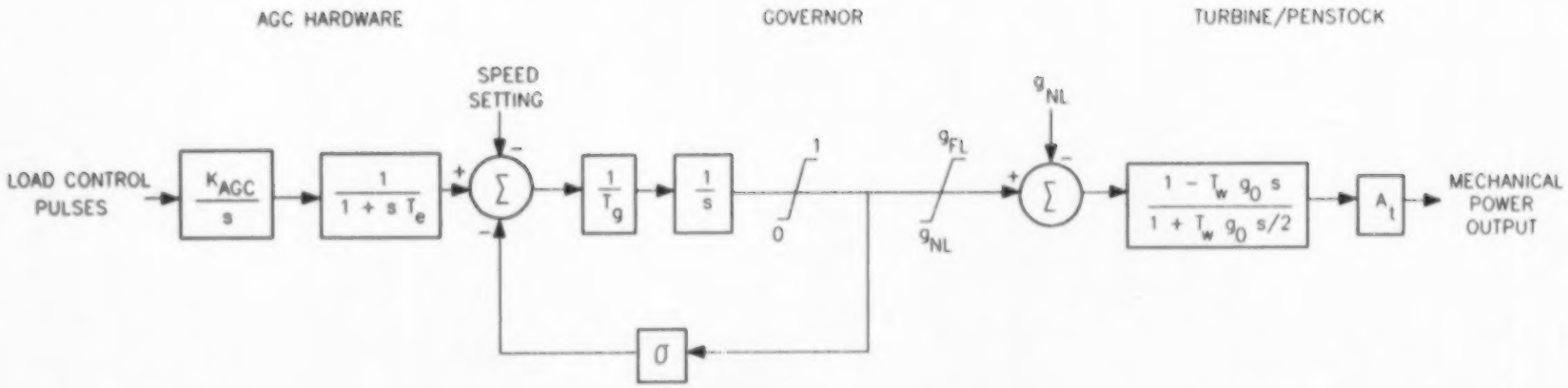

FIGURE 25 : SIMPLIFIED TRANSFER FUNCTION BLOCK DIAGRAM FOR AGC OPERATION AT S.A.BECK II GS

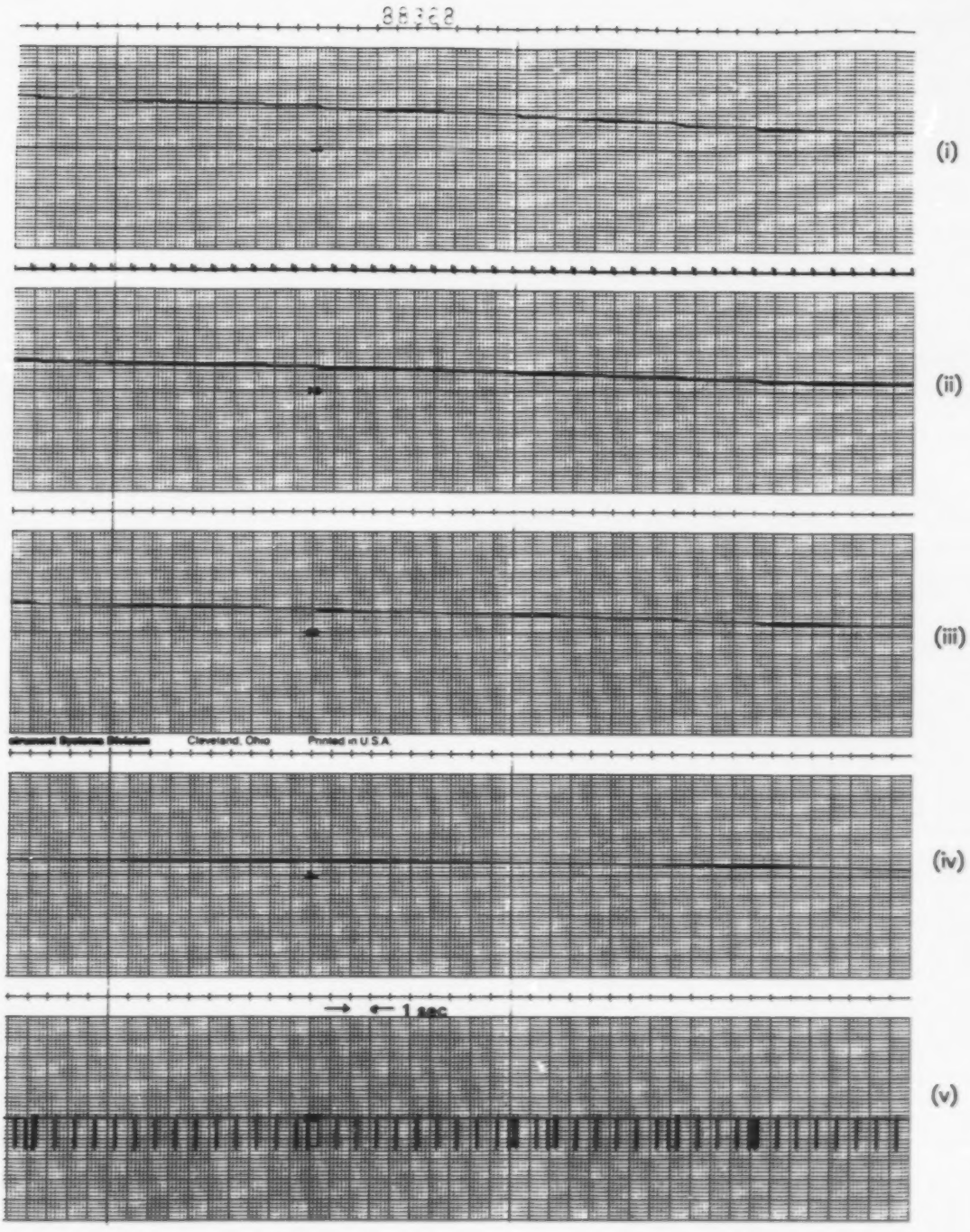

FIGURE 26 – AGC QUANTITIES RECORDED MORNING OF MARCH 10,1987

(i) MOS OUTPUT (100 mV FS)
(ii) TRANSMITTER 1 OUTPUT (50 mA FS)
(iii) TRANSMITTER 2 OUTPUT (50 mA FS)
(iv) TOTAL PLANT OUTPUT (2000 MW FS)
(v) LOWER PULSES

DISTRIBUTION

Dr. D. Mills	Director of Research
Mr. A.J. Harris	Power System Operations, A6-H1
Mr. D. Barrie	Power System Operations, A6-H13
Mr. C.E. Graham	Power System Operations, A6-A13
Mr. P.D. Henderson	Power System Operations, A6-H12
Dr. H.M. Zein El-Din	Power System Operations, A6-A12
Mr. M.E. Coultes	Power System Operations, Richview SCC
Mr. L.J. Rubino	System Planning, H4-G25
Dr. P. Kundur	System Planning, H5-J21
Dr. A.S. Morched	System Planning, H5-J20
Mr. G.J. Rogers	System Planning, H5-G21
Mr. D.G. Rishworth	Design & Development - Transmission, H10-B22
Mr. M.T. McPhedran	Design & Development - Generation, H13-D12
Mr. T.H. Warburton	Thermal & Hydraulic Generation, A12-A18
Mr. A.M. Wilson	Thermal & Hydraulic Generation, A14-H14
Mr. R.A. Wright	Thermal & Hydraulic Generation, A12-A14
Mr. R. Storey	Technical & Training Services, A8-H4
Mr. R.R. Urquhart	Transmission Operation, U3-A5
Mr. F.M. Gram	Western Region
Mr. J. Newbold	Western Region
Mr. A.F. Baljet	Electrical Research, KR120
Mr. D.C. Lee	Electrical Research, KR132
Mr. R.E. Beaulieu	Electrical Research, KR132
Mr. G. Manchur	Electrical Research, KR134
Mr. G.R. Bérubé (2)	Electrical Research, KR134

Public Reference Centre
Editorial Section
Office Copies (2)
Extra Copies (2)